IDENTIFYING SEDIMENT SOURCE AREAS IN A MEDITERRANEAN WATERSHED USING THE SWAT MODEL

Abstract

This study aims to evaluate the suitability of the Soil and Water Assessment Tool (SWAT) model in simulating runoff and sediment loss in the Carapelle (SE Italy), a typical Mediterranean watershed, where continuous measurements of streamflow and sediment concentration were collected over a five-year period, on a half-hour timescale, processed on a daily timescale. After sensitivity analysis, the model was calibrated, and validated for runoff and sediment. Statistics show generally satisfactory efficiency. To further improve sediment simulation performance, we used a seasonal calibration scheme, in which data recorded in the dry and wet seasons were used to calibrate sediments separately, on a seasonal basis. We also tested the model's capability in identifying the major sediment source zones, and river segments where there is sediment deposition. On the basin scale, the average water yield (186mm) corresponds to 27% of the total rainfall (686mm) and average annual sediment load was estimated to be 6.8 t ha^{-1} yr^{-1}. On the sub-basin scale, a gradient of sediment yield was found that is characterised by a large difference among the upper (7 to 13 t ha^{-1} yr^{-1}), central, and lower parts (<1 t ha^{-1} yr^{-1}) of the study area. Conversely, deposition in channel flow has its highest values in the central part of the watershed, where there is an alluvial plain. Winter wheat and olive landuse are the major source areas, in terms of sediment. This study confirms that the Mediterranean watershed is a fragile ecosystem, and measures are needed to mitigate soil depletion.

Keywords: SWAT model; sediment calibration; sediment yield; sediment source areas; Mediterranean watershed

Authors:

Ricci, Giovanni Francesco
University of Bari Aldo Moro, Department of Agricultural and Environmental Sciences
Mail: giovanni.ricci@uniba.it

De Girolamo, Anna Maria
National Research Council, Water Research Institute (CNR-IRSA), Bari, Italy
Mail: annamaria.degirolamo@ba.irsa.cnr.it

Abdelwahab, Ossama.M.M;
Cairo University Faculty of Agriculture, Department of Agricultural Engineering;
Mail: el.khwaga_eng@yahoo.com

Gentile, Francesco;
University of Bari Aldo Moro, Department of Agricultural and Environmental Sciences
Mail: francesco.gentile@uniba.i

Corresponding author
Ricci, Giovanni Francesco
Mail: giovanni.ricci@uniba.it

1. Introduction

Land degradation, in its various forms, is a common problem in Europe (Panagos *et al*., 2014) and in many other parts of the world (European Commission, 2006; Jones *et al*., 2012; Garcìa-Ruiz *et al*., 2016). Although soil has a fundamental role in ecosystems and economies (Pimentel, 2006; Tibebe & Bewket, 2011), it is perceived to be abundant and, as its degradation is generally a slow process, it passes unnoticed. In order to increase awareness regarding the soil erosion problem and its impact on water quality, ecosystem services, biodiversity, and food production, the European Commission (2006) listed erosion among the soil risks in their Soil Thematic Strategy (http://ec.europa.eu/environment/soil/index_en.htm), and identified measures that the member states needed to take to combat soil threats.

Watershed management can play an important role in protecting soil and water (Nikolaidis *et al*., 2013; Abdelwahab *et al*., 2014; Bisantino *et al*., 2015); however, before identifying specific conservation and best management practices (BMPs) in order to mitigate soil depletion, there is a need to quantify erosion and identify the source zones of such sediment in the watershed (Asres & Awulachew, 2010; Abdelwahab *et al*., 2016; Vigiak *et al*., 2016).

Sheet and rill erosion are the most widespread types of accelerated water erosion in Europe (Panagos *et al*., 2015), constituting the principal cause of land degradation (Garcìa-Ruiz *et al*., 2016). Soil sediments detached from the agricultural watershed landscape due to water erosion carry nutrients, fertilisers and chemicals that reach water bodies and lead to water quality impairment (Rickson *et al*., 2014; Gamvroudis *et al*., 2015). Additionally, the sediment regime exerts a great influence on aquatic and riparian ecosystems (Wohl *et al*., 2015).

On a basin scale, sediment yield is the result of several factors controlling runoff generation and erosion processes, and it is strongly related to factors controlling the sediment dynamics in a catchment, including sediment generation, transport and deposition (Parsons, 2012). Indeed, the shape of a given hillslope, and its natural or artificial geomorphological features, may exert a substantial influence on erosion and deposition (Fryirs *et al*., 2007), as well as on connectivity (Fryirs, 2013) and pathway development (Marchamalo *et al*., 2016). The term ‘connectivity’ is used to describe the extent to which sediment generated on hillslopes is connected to a channel, by overland and subsurface flow, as well as the linkage of streamflow and sediment within a channel network (Hooke, 2003; Lesschen *et al*., 2009; Medeiros *et al*., 2010; Di Stefano & Ferro, 2017). Erosion and connectivity are complex and non-linear processes that involve a large number of factors that cannot be monitored directly. Spatial and temporal variability of physical processes causing erosion and sediment delivery poses a severe limitation both on field measurements and for up-scaling results of field measurements, especially in semi-arid landscapes (Marchamalo *et al*., 2016). For these reasons, soil loss assessment is generally performed by means of models (Collins & Walling, 2004).

In recent decades, a large number of erosion models have been developed, operating at different time and spatial scales with various levels of complexity (Ferro & Porto, 2009; Cerdà *et al*., 2010; Karydas *et al*., 2014). Among these models are the Water Erosion Prediction Project (WEPP: Flanagan *et al*., 2012), Annualized Agricultural Non-Point Source (AnnAGNPS: Theurer & Cronshey, 1998; Bingner & Theurer, 2005; United States Department of Agriculture - Agricultural Research Service [USDA-ARS], 2011), Agricultural Policy Environmental eXtender (APEX: Gassman *et al*., 2010), European Soil Erosion Model (EUROSEM: Morgan *et al*., 1998), Kinematic Runoff and Erosion Model (KINEROS2: Smith *et al*., 1995), Pan European Erosion Risk Assessment (PESERA: Kirkby *et al*., 2003), Revised Universal Soil Loss Equation (RUSLE2015: Panagos *et al*., 2015), and the Soil and Water Assessment Tool (SWAT: Arnold *et al*., 1998).

Although they are efficient as decision support tools, one of the limiting factors of most hydrological models is that they require a large number of spatially and temporally variable input data (Abouabdillah *et al*., 2014). Additionally, model results are affected by uncertainties with regards to the conceptual model, input and parameterisation, which can complicate performance (Pappemberg

& Beven, 2006, Abbaspour *et al*., 2007; Refsgaard *et al*., 2007; Gotzinger & Bardossy, 2008; Yang *et al*., 2008; Abbaspour *et al*., 2015)

The SWAT model is one of the most widely used semi-distributed models for evaluating erosion and sediment transport processes, allowing simulation of dominant sediment sources (Oeurng *et al*., 2011; Bonumá *et al*., 2012; Furl *et al*., 2015; Krysanova & White, 2015; Vigiak *et al*., 2015); however, recent studies (Table I) have identified difficulties in simulating hydrology and sediment load in regions under Mediterranean climates, according to the Koppen (1931) classification of: Mediterranean basin, coastal California, southern Australia, South Africa and central Chile. The absence of streamflow, which is frequently recorded in the river networks of these regions, is a critical point in model hydrological simulations (De Girolamo *et al*., 2017). Moreover, a few studies reported SWAT applications to simulate sediment load in Mediterranean basins with temporary river systems (Gamvroudis *et al*., 2015), with particular reference to sediment modeling on a daily timescale (Licciardello *et al*., 2011). Generally, sediment calibration and validation is performed on a monthly basis (Table I), and the results, which are presented on a yearly to monthly basis, show an underestimation of sediment load. Nevertheless, in medium or small watersheds, a large difference can be found between daily and monthly values, in terms of sediment load, therefore a monthly timescale is not exhaustive for analysing erosion and sediment delivery processes in these watersheds. Mediterranean rivers exhibit a specific hydrological regime, characterised by extremely low flow with flash flood events (Bisantino *et al*., 2010; Skoulikidis *et al*., 2017), which complicates both monitoring and modeling activities (Oueslati *et al*., 2015; De Girolamo *et al*., 2017). Although measurements of streamflow and sediment concentration on a daily timescale are fundamental for river research and watershed management, monitoring surface waters remains a challenge in the Mediterranean region.

In this context, the aims of the present study were to: (i) evaluate SWAT model suitability in simulating runoff and sediment loss in the Carapelle (SE Italy), a typical Mediterranean watershed, where continuous measurements of streamflow and sediment concentration were collected over a five-year period, on a half-hour timescale, successively processed on a daily timescale; (ii) identify a strategy for improving sediment load simulation in streams characterised by extremely low flow; and (iii) assess model capabilities in the evaluation of sediment connectivity, by identifying source zones and sediment deposition along the channel in the watershed, in order to address where a program of measures can be implemented to mitigate soil erosion.

Dealing with a streamflow and sediment load simulation in a typical watershed under Mediterranean climate, we tried to analyse and discuss what water resources managers can expect from hydrological models, and the problems that modelers have to acknowledge and overcome. The approach tested in this paper for sediment calibration, as part of the global model calibration, despite being specific to the SWAT model, is applicable to different models, and to other basins characterised by extreme low flow and high temporal variability in streamflow, such as the Carapelle.

Table I. A selection of relevant studies performed on the Mediterranean climatic region (classification of Koppen, 1931), concerning sediment load simulation with the SWAT model (this paper included).

Related case studies	Study area	Calibration and Validation Period and time step	Key results
Potter & Hiatt., 2009	California	Few a year grab sample measurements Calibration 2005 - 2007	Average annual sediment load 3.66 t ha^{-1} yr^{-1} SWAT model generally tends to underestimate the measured sediment PBIAS for three gauge station: + 52.6; +26.5 and +73.9
Gamvroudis *et al*., 2014	Greece	Monthly time step Calibration 2010 - 2011	Average annual sediment yield 0.85 t ha^{-1} yr^{-1} In the two main flood event SWAT, simulate suspended sediment appropriately with a slight underestimation. PBIAS for two gauging station: +33.4 and +13.4
Nerantzaki *et al*., 2015	Greece	Monthly time step Calibration: 2011 - 2014	Average erosion rate from 0.97 t ha^{-1} yr^{-1} to 1.6 t ha^{-1} yr^{-1} Model overestimation due to the fact that the majority of the observations had low values of sediment concentration PBIAS -57%
Peraza-Castro *et al*., 2015	Northern Spain	Daily time step Calibration 2009 - 2012 Validation 2001 - 2009	Average annual sediment load 0.33 t ha^{-1} yr^{-1} Underestimation and overestimation during some flood events. The underestimation occurs for four events that according to Montoya-Armenta (2013).
Briak *et al*., 2016	Northern Morocco	Monthly time step Calibration 1976 - 1984 Validation 1985 - 1993	Average annual sediment yield 55 t ha^{-1} yr^{-1} Generally SWAT tends to underestimate peak of sediment concentration PBIAS +7.12 for calibration; PBIAS +15.51 for validation
Gyamfi *et al*., 2016	Southern Africa	Monthly time steps Calibration 1994 - 1995 Validation 1996 - 1997	Mean sediment yield for the Land use change scenario varies from 1.33 t ha^{-1} yr^{-1} to 4.46 t ha^{-1} yr−1. Simulated sediment match fairly with the observed with an underestimation PBIAS + 27.36 for calibration; PBIAS +39.73 for validation
Chen *et al.*, 2017	California	Monthly time step Calibration 2003 - 2008 Validation 2009 - 2014	Model significantly overestimate sediment load during peak events with default Bagnold equation, but produced better results when the physically based Bagnold equation is used. PBIAS - 32 for Calibration; PBIAS 0 for Validation
This Work	Southern Italy	Daily and Monthly time step Calibration 2007-2008 Validation 2009 - 2010	Average annual sediment load 6.8 t ha^{-1} yr^{-1} SWAT model showed generally an overestimation of the dry season and an underestimation of the wet season

2. Materials and methods

2.1 Study area

The Carapelle watershed (Figure 1) is located in northern Apulia (SE Italy). The drainage area is 506 km^2 and the main channel length is 52.16 km. The watershed is characterised by a mean elevation of 466 m above sea level (asl), varying between 120 and 1089 m asl. The mean watershed slope is 8.2%, and the mean slope of the main channel is 1.8%.
The river headwaters are in the neighboring Campanian Apennine region, and most of the upper watercourse crosses the orographic system of the Daunia Hills (Abdelwahab *et al*., 2013). The channel is confined to the hilly part of the basin, and assumes a braided form in the alluvial plain, where the coarser material is deposited. The hydrological regime is characterised by high variability over a short time, with extremely low flow conditions during the summer months (June to September) and high flow conditions recorded in winter and early spring.

Sheet wash and concentrated water erosion are the main active erosion processes in the area, with no noticeable form of gully erosion. In addition, several landslides are present in the area, where the geological units (clay-flysch: http://93.51.158.165/POR/map_default.phtml) are susceptible to slope movement mainly related to rainfall events (Wasowski *et al*., 2007). Bank erosion is also an active process, especially in the upstream river reaches.

Mediterranean climatic conditions prevail in the watershed, with wet autumn/winter and dry spring/summer seasons (Milella *et al*., 2012). Precipitation ranges from 450 to 800 mm y^{-1}, and the rainiest months are March and November, while August is the driest.

The monitoring station, which is located near the village of Ordona (41°17'50.347"N, 15°36'2.583"E), is equipped with two gauging systems. For measuring streamflow, the Puglia Region Technical Service (National Hydrographic Service) provides an electromechanical and ultrasound stage meter that registered data every half an hour. An infrared optical probe (Hach-Lange Solitax) was used for measurements of suspended sediment concentration (SSC) at half-hour intervals. The streamflow and SSC measurements were processed in order to obtain daily sediment loads over the whole study period (2007-2011), with only a few weeks interruption for maintenance. A complete description of the gauging station and equipment can be found in Gentile *et al.* (2010). The highest

SSC recorded in the study period is 47.83 g L^{-1}, corresponding to a peak flow of 19.82 $m^3 s^{-1}$ (Garcìa-Rama *et al*., 2016).

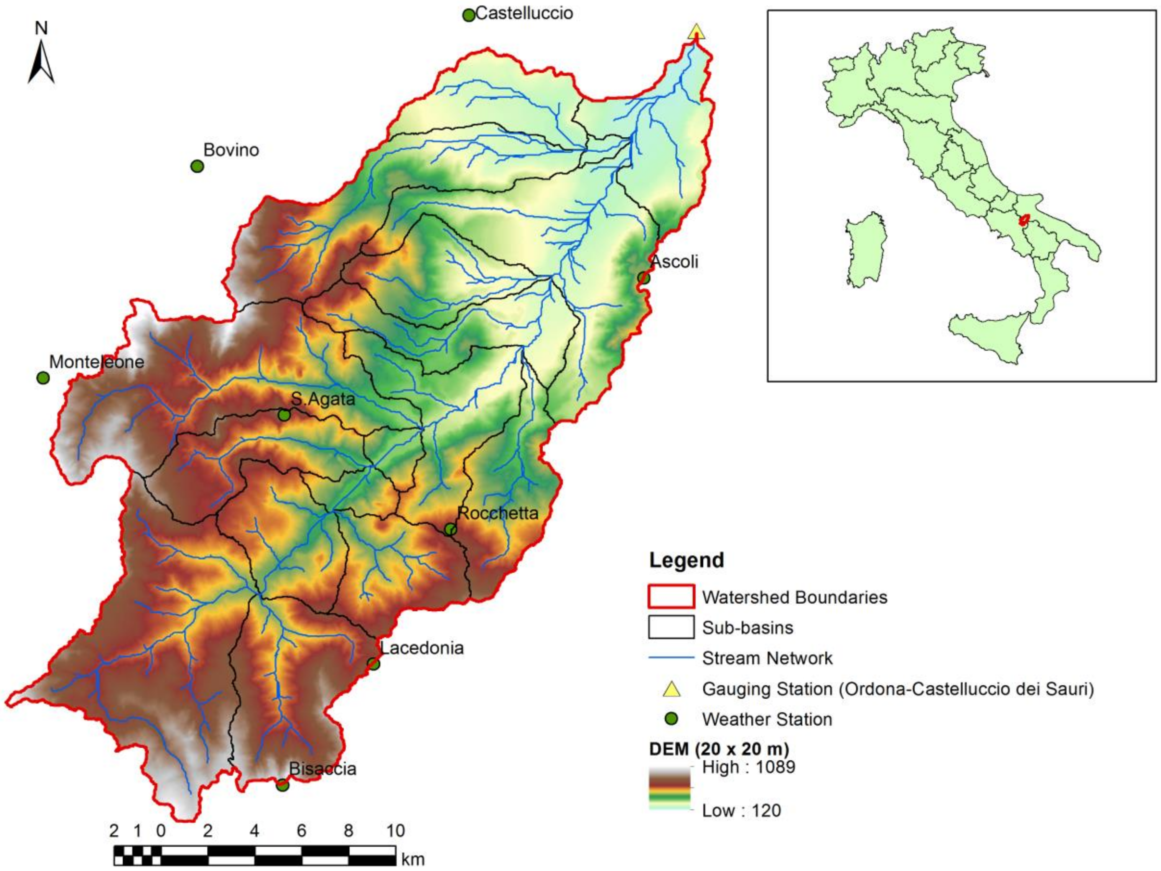

Figure 1. Study area: the Carapelle watershed (Apulia region, SE Italy).

2.2 Model configuration

The SWAT2012 version with Arc-GIS interface (Winchell *et al*., 2013) was run from 2007 to 2011, using a daily interval, with two years of warm up (2005-2006). SWAT is a semi-distributed, continuous hydrological model (Arnold *et al*., 1993; Arnold *et al*., 1998) that was developed for assessing the long-term impacts of different conservation and management practices on water bodies in ungauged catchments (Srinivasan *et al*., 1998; Arnold *et al*., 2012; Glavan *et al*., 2013). The history of the model can be found on http://www.brc.tamus.edu/swat/ and a review of recent developments and applications has been reported in Volk *et al*. (2016).

For simulation of the physical processes associated with water and sediment, the SWAT model divides the watershed into sub-basins and, further, into hydrological response units (HRU) that are areas with homogenous slope, land use, management and soil characteristics. In our study, the watershed was discretised by setting the upstream drainage area, which is required to define the beginning of a stream, to 2000 ha, resulting in 17 sub-basins. A percentage threshold of land use, soil class, and slope were then set to 10%, 10%, and 20%, respectively, resulting in 87 HRUs. We verified that, with these thresholds, only minor land uses and soils were eliminated, and that the original proportion of land use and soil within each sub-basins was maintained. Extra caution was used to ensure that areas with high potential erosion were not excluded from these thresholds.

Hydrological balance is considered to be the driving factor, as it affects all physical processes in the watershed, including plant growth, chemicals and sediment routing (Arnold *et al*., 2012). The model simulates hydrology in two separate phases: the landscape phase, which controls the quantity of water, sediment, nutrients and pesticides moving from each sub-basin towards the main stream; and the in-stream phase, which controls the movement of water and sediments in the stream system towards the watershed outlet. Surface runoff is estimated using the modified Soil Conservation Service-Curve Number (SCS-CN) method (USDA-SCS, 1972), and Manning's equation is used to predict stream velocity and discharge. Erosion in SWAT is computed using the Modified Universal Soil Loss Equation (MUSLE: Williams, 1975), which determines sediment yield using the same parameters as the original USLE, except that the rainfall erosion factor is replaced by a runoff factor. The entire estimated amount of eroded sediment in the hillslope areas reaches the channel (Le Roux *et al*., 2013). The model considers most connectivity aspects in one simulation package, including factors controlling upland sediment generation, channel transport, and sediment deposition (Collins & Walling, 2014). For channel sediments, SWAT simulates the two dominant sediment transport processes of degradation and deposition (Neitsch *et al*., 2002), with a simplified version of the Bagnold stream power relationship (Bagnold, 1977), where the maximum transport is based on the peak channel velocity. The Hargreaves Method was chosen to evaluate potential evapotranspiration (Hargreaves, 1975), since temperature and solar radiation values were available for the study area.

The SWAT model generated several output files and results aggregated at different levels: basin, sub-basin, river segment (reach), and HRU. The SWAT model does not consider the processes of deposition during transport from the HRU to the channel. Hence, an entire sub-basin is identified as a source of sediment; however, by processing the in- and out-variables generated by the model, it is possible to identify the reaches where there is sediment deposition, and the critical HRUs in terms of soil loss.

2.3 Input data

A Digital Elevation Model (DEM), with a resolution of 20×20 m, was used to delineate the watershed. Land use data are based on a merge between the Land Use Map of Apulia and the Land Agricultural Use Map of Campania, both with a resolution of 100 m, obtained from the geoportals of both regions. The land use is largely represented by winter wheat (76%), with a lower fraction of deciduous forest (7%), coniferous forest (4%), olive orchard (3.3%), rangeland (7%), and other land uses. All classes were reclassified, according to the Corine Land Cover classes (European Environment Agency, 2006), and a SWAT code was then assigned to each land use to create the land use database.

Currently, soil data with high resolution, covering the whole basin, are not available. Hence, the soil data attributes were extracted from the topsoil physical properties for European maps (Ballabio *et al*., 2016) that were provided by the European Soil Data Centre (ESDAC), based on the Land Use and Cover Area Frame Statistical survey (LUCAS) data, a project aimed at collecting homogenous data about the state of land use/cover across the European Union (Tóth *et al*., 2013). Through a GIS-based process of overlaying different maps (texture, coarse fragment, bulk density, organic carbon, and available water capacity), a layer that gathered all soil characteristics was obtained, with a resolution of 500 m. Five soil textures were identified, with clay loam texture representing almost 48% of the watershed area. Soil profiles were identified using the Soil Profile Analytical Database for Europe (SPADE/2: Hiederer *et al*., 2006), creating a link between the database and a map of soil polygons from the Soil Geographic Database of Europe (SGDBE).

Climate data (e.g. daily maximum and minimum temperatures, daily precipitation), acquired by eight weather stations located in the watershed and its surroundings, were used as the input climate data for the simulations. The management operation data, regarding winter wheat and olive, were collected from field surveys and farmer interviews. Planting, harvesting, and tillage applications were simulated for each cropping system with specific dates. For winter wheat, a four-year crop rotation was adopted, with plowing (25-40 cm) in August, harrowing in October, and three fertilisations in December, February, and April. In order to take into account the actual agricultural practices (deep and up and down plowing), the SWAT2012.mdb was modified with a new value for depth (400 mm). The crop was planted in November and harvested in July. For olive plants, on the other hand, three shallow tillages (plowing and harrowing) occurred every two months, starting in April, two organic fertilisations were applied in December and January, and the plants were harvested in November (Abdelwahab *et al*., 2016).

2.4 Model calibration and validation

The automated software SWAT-CUP (Abbaspour *et al*., 2015) was used to perform a global sensitivity analysis, in order to remove insensitive parameters from the calibration process. A t-test was used to identify a measure of sensitivity (i.e. larger absolute values imply higher sensitivity) of each hydrological and sediment parameters (Arnold *et al*., 2012), and *p*-values were used to determine the significance of the sensitivity, by testing the null hypothesis where the coefficient is equal to zero or, in other words, where the parameter has no effect (e.g. a p-value < 0.05 means that there is only 5% probability that results would generate a random distribution) (Swiss Federal Institute of Aquatic Science and Technology [EAWAG], 2013). At the end of the sensitivity analysis, the 10 most sensitive parameters for runoff and four parameters for sediment were chosen to be analysed thoroughly in a model calibration process.

The observed data for runoff and sediment load were collected from 2007 to 2011, on a daily timescale. In order to perform a runoff calibration and validation, the observed streamflow data were split into two periods (Gan *et al*., 1997). Hence, the calibration was performed for the years 2007-2008, with validation for the period 2009-2011. The years selected for calibration and validation are representative of annual and inter-annual variability, in terms of rainfall, streamflow, and sediment load. A very dry spring and summer were recorded in 2007 and 2010 (e.g. precipitation in August 0.47 mm in 2007; 0.72 mm in 2010). A very rainy November and December were recorded in 2008, 2009, and 2010.

Automatic calibration and parameter uncertainty analysis was performed for streamflow by applying Sequential Uncertainty Fitting v.2 (SUFI-2) on a daily timescale, using SWAT-CUP to search for parameter values that optimised an objective function, such as the Nash & Sutcliffe (1970) efficiency (NSE) value (Gupta *et al*., 1999). Before starting the automatic calibration process, the type of change to be applied to the parameter was selected (EAWAG, 2013). In particular, to reflect physical factors such as soil type, land use, elevation, and their spatial variability, for CN and available water capacity (SOL_AWC), it was chosen to maintain the spatial variability, and the initial fixed value for HRU was multiplied by a 1+a given value (letter R in Table II). For the other parameters, the initial fixed value was replaced by a given value (letter V in Table II).

Subsequently, the model was calibrated for sediment load, as recommended by several studies (Santhi *et al*., 2001; Engel *et al*., 2007; Arnold *et al*., 2012). A manual calibration at daily intervals was preferred in this case, due to the reduced number of parameters (four) evidenced by the sensitivity analysis (Table II). The calibration was carried out for a period of two years (2007-2008) maintaining fixed runoff parameters. By changing sediment parameters one at a time, and for the whole basin, a range of values was considered for each parameter, and the best simulation was fixed, based on the maximum objective function (NSE).

To evaluate the model efficiency, we used the coefficient of determination (R^2), NSE, and the percent bias (PBIAS). The obtained R^2 values show the degree of collinearity between simulated and measured data. The NSE determines the relative magnitude of the residual variance, compared to the variance of the measured data. The PBIAS measures the average tendency of the simulated data to be larger or smaller than the measured data (Gupta *et al*., 1999). Acceptable values are considered as NSE > 0.5, $R^2 > 0.5$, and PBIAS ± 25 for runoff and ± 55 for sediment, as suggested by Moriasi *et al*. (2007). Other authors (e.g. Zema *et al*., 2016) considered a value of NSE > 0.35 to be satisfactory in Mediterranean areas.

Another step was the evaluation of the model performance, by splitting all the daily and monthly values into two periods, one corresponding to the wet season (from October to April) and the other the dry season (from May to September). After that, a new calibration for sediment was performed on a seasonal basis.

3. Results

3.1 Modelling

The most sensitive parameters for runoff and sediment and the corresponding t-Stat and *p*-value used in the model calibration process are showed in Table II.

After 1000 iterations, SWAT-CUP identified a range of values for each parameter included in the sensitivity analysis, based on the maximum objective function, which in this case was the NSE. Using these ranges, SWAT-CUP simulated a 95% probability distribution (95PPU), which was calculated at 2.5% and 97.5% of the cumulative distribution of results (Abbaspour *et al*., 2015), yielding the best fit value corresponding to the set of parameters that gives the best estimation curve (Table II). The results of the uncertainty analysis, using the SUFI-2, are shown in Figure 2, which illustrates the best simulation, the observed streamflow, and the 95PPU. As shown in Figure 2, the uncertainty interval is quite large under both high and low flow conditions. These results are consistent with the studies of Uhlenbrook *et al*. (1999) and De Girolamo *et al*. (2017).

Table II. SWAT sensitivity analysis results, default range of parameters and best-fit calibration. Letter R is for relative change (initial parameter is multiplied by 1+ a given value in calibration). Letter V is for replacement (initial parameter is replaced by a given value).

Parameters	Description	t-Stat	p-Value	Range	Best fit
	Runoff				
V__ESCO.hru	Soil Evaporation compensation factor	174.459	0.000	0.83-1.00	1.000
R__CN2.mgt	Curve Number	145.900	0.000	0.04-0.11	0.080
V__ALPHA_BF.gw	Baseflow alpha factor	88.771	0.000	0.38-0.75	0.460
V__GWQMN.gw	Threshold depth of water in shallow aquifer	1.399	0.162	0.19-0.40	0.300
V__GW_REVAP.gw	Groundwater "revap" coefficient	0.934	0.351	0.03-0.14	0.060
V__CH_N2.rte	Manning's "n" value for main channel	-4.374	0.000	0.01-0.03	0.010
V__CH_K2.rte	Effective hyd. Cond. In the main channel	-17.760	0.000	38.70-42.90	40.910
V__GW_DELAY.gw	Groundwater delay time	-33.269	0.000	31.11-70.37	35.600
V__OV_N.hru	Manning's "n" value for overland flow	-42.025	0.000	7.51-12.54	12.510
R__SOL_AWC.sol	Soil available water storage capacity	-61.333	0.000	0.39-0.57	0.560
	Sediment				
ADJ_PKR.bsn	Peak rate adjustment factor for sediment routing in the sub-basin	0.087	0.931	-	1.400
LAT_SED.hru	Sediment concentration in groundwater flow	-0.643	0.520	-	250.000
SPCON.bsn	Maximum amount of sediment reentrained during channel sediment routing	-0.672	0.502	-	0.003
BIOMIX.mgt	Biological mixing efficiency	-0.785	0.432	-	0.500

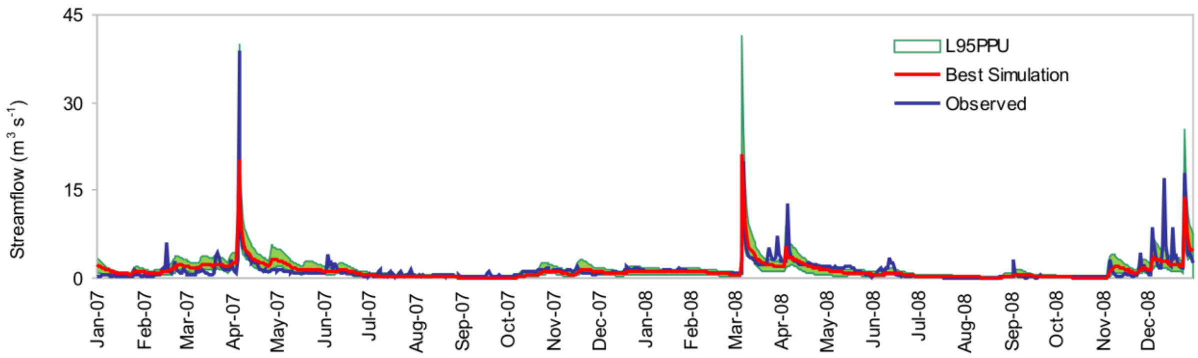

Figure 2. Observed daily streamflow, 95% model uncertainty, and best simulation at the outlet. Calibration period: 2007-2008.

The daily sediment calibration (2007-2008) results (i.e. best fit simulation and uncertainty interval) are reported in Figure 3. Daily sediment validation was carried out for a three-year period (2009-2011).

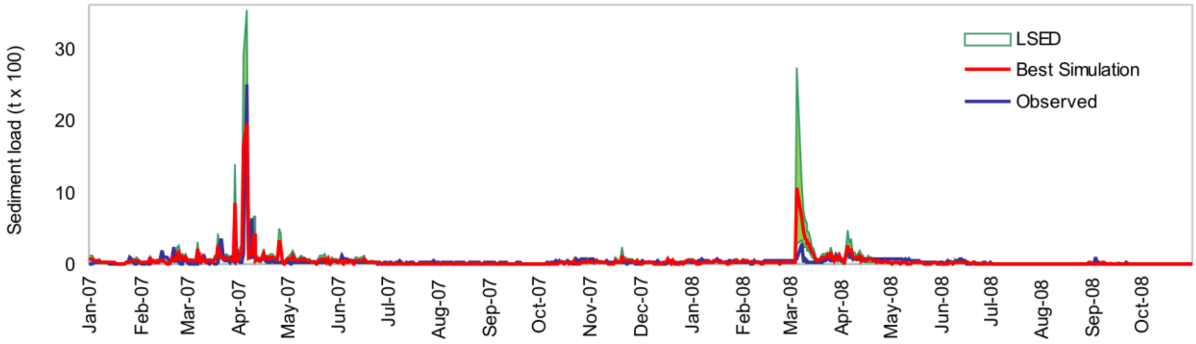

Figure 3. Daily observed and simulated sediment, model uncertainty, and best simulation at the outlet. Calibration period: 2007-2008. Daily sediment calibration for period 2007-2008.

The goodness of fit between the modeled and observed data for the calibration period was evaluated using the NSE, R^2 and PBIAS indices. Statistical index values are shown in Table III, both for the calibration and validation periods. The values obtained for daily streamflow and sediment calibration showed satisfactory model efficiency, according to Moriasi *et al*. (2007), while those obtained for the validation period should be considered not satisfactory according to the same Authors (Table III). On a monthly timescale the values can be considered satisfactory according to Moriasi *et al*. (2007) and Zema *et al*. (2016) both for calibration and validation.

To better investigate results obtained from the calibration and validation, all daily values were split into two periods, one corresponding to the wet season (October to April) and the other to the dry season (May to September). All were then statistically reconsidered. The results (Figure 4) revealed that the model tends to perform better in the wet season, compared to the dry season, both for runoff and sediment simulations. In particular, upon evaluating the model performance on a monthly scale, runoff showed good performance (NSE = 0.7, R^2 = 0.6, PBIAS = 3.6) in the wet season, while it was unsatisfactory in the dry season (NSE = -0.3, R^2 = 0.7, PBIAS = -43.3), for which an overestimation was revealed. After an accurate analysis of the dry period, which included rainfall, measured and simulated streamflow, it was evident that the low performance was mainly due to few flood events occurred in 2010 due to convective rainfalls. In these cases, to enhance SWAT simulation results, Moon *et al*. (2004), Kalin & Hantush (2006) suggest to use Next-Generation Weather Radar (NEXRAD) precipitation. Unfortunately, in Carapelle watershed these kind of data were not available. However, a check was done to evaluate the performance of the model without these three events. The results in terms of statistics were satisfactory, hence based on this evidence a calibration based on a seasonal scheme was not carried out.

Monthly sediment simulations showed similar good results in the wet season (NSE = 0.6, R^2 = 0.7, PBIAS = -28.2). In the dry period, the model performance was unsatisfactory (NSE = 0.1, R^2 = 0.2, PBIAS = +69.0); however, in this case, an underestimation of the data was indicated.

Based on these results, a new calibration of sediment load was performed, differentiating between the dry and wet seasons. In particular, as the streamflow varied from extremely low (0.010 $m^3 s^{-1}$) to high (60 $m^3 s^{-1}$), a combination of two different values of the linear parameter for calculating the maximum amount of sediment that can be re-entrained during channel sediment routing (SPCON) (Table II) for the dry and wet periods was found to perform better channel sediment routing in the Carapelle river system. The initial range of this parameter (0.0001-0.01) was restricted to a smaller interval of variability (0.0008-0.005). In particular, while the best value for the whole hydrological year, in terms of statistical performance, was 0.003, two different optimal values were identified for the dry (0.0008) and wet (0.005) seasons. With this strategy, the results improved, in terms of statistical indices, as listed in Table III, while it was found that, by using the values 0.0008 and 0.005, for the whole period, PBIAS was +77.78 and -53.65, respectively.

Table III. Model performance statistics for annual calibration/validation and for seasonal calibration (wet/dry periods).

Daily	0.6	0.6	-1.0	0.4	0.4	2.0
Monthly	0.9	0.8	12.5	0.6	0.6	-14.3
Sediment						
Daily	0.6	0.6	-1.5	0.2	0.2	29.5
Monthly	0.7	0.5	-0.6	0.7	0.7	-5.3
	Wet			Dry		
Runoff						
Daily	0.5	0.5	1.6	0.4	-1.4	-39.8
Monthly	0.6	0.7	-3.6	0.7	-0.3	-43.3
Sediment						
Daily	0.5	0.5	17.3	0.2	-3.7	-140.1
Monthly	0.7	0.6	-28.2	0.2	0.1	69.0
Sediment with new calibration						
	Wet (SPCON 0.005)			Dry (SPCON 0.0008)		
Daily	0.5	0.6	-38.4	0.5	0.5	33.9

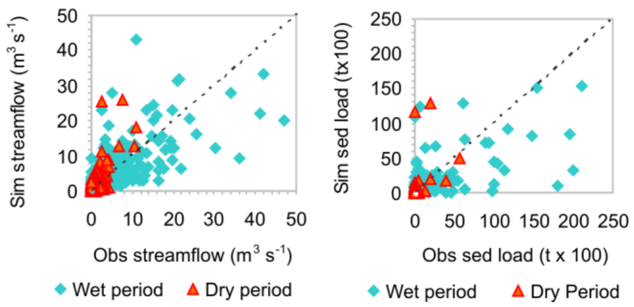

Figure 4. Simulated daily streamflow versus observed daily streamflow for the wet (NSE = 0.45, R^2 = 0.5, PBIAS = +1.58) and dry (NSE = -1.42, R^2 = 0.35, PBIAS = -39.83) seasons (a); simulated daily sediment load versus observed daily sediment load for the wet (NSE = 0.5, R^2 = 0.5, PBIAS = +17.26) and dry (NSE = -3.73, R^2 = 0.2, PBIAS = -140.06) (b) seasons.

In order to evaluate the efficiency of the new calibration, all the flood events were analysed in terms of peak discharge and sediment load. In Figure 5a three events with different intensities (14th October, 2010; 19th February, 2011; 5th March, 2011) are represented. By using SPCON = 0.003 (best value for whole period); the observed sediment load is generally underestimated. As the Figure 5a shows , observed sediment load was 10341 t, 35914 t, and 64281 t in October, February, and March, respectively, while simulated load was 4245 t, 49294 t, and 30508 t, respectively. In the same way, by using a SPCON = 0.005, sediment load for the three events became 11306 t, 37226 t, and 68875 t, respectively. Analysing the dry period (Figure 5b) (from May to July, 2007), it is evident that observed sediment load is overestimated, by using the best value for the whole period. An improvement of fit was obtained by using the value calibrated specifically for the dry period (SPCON = 0.0008).

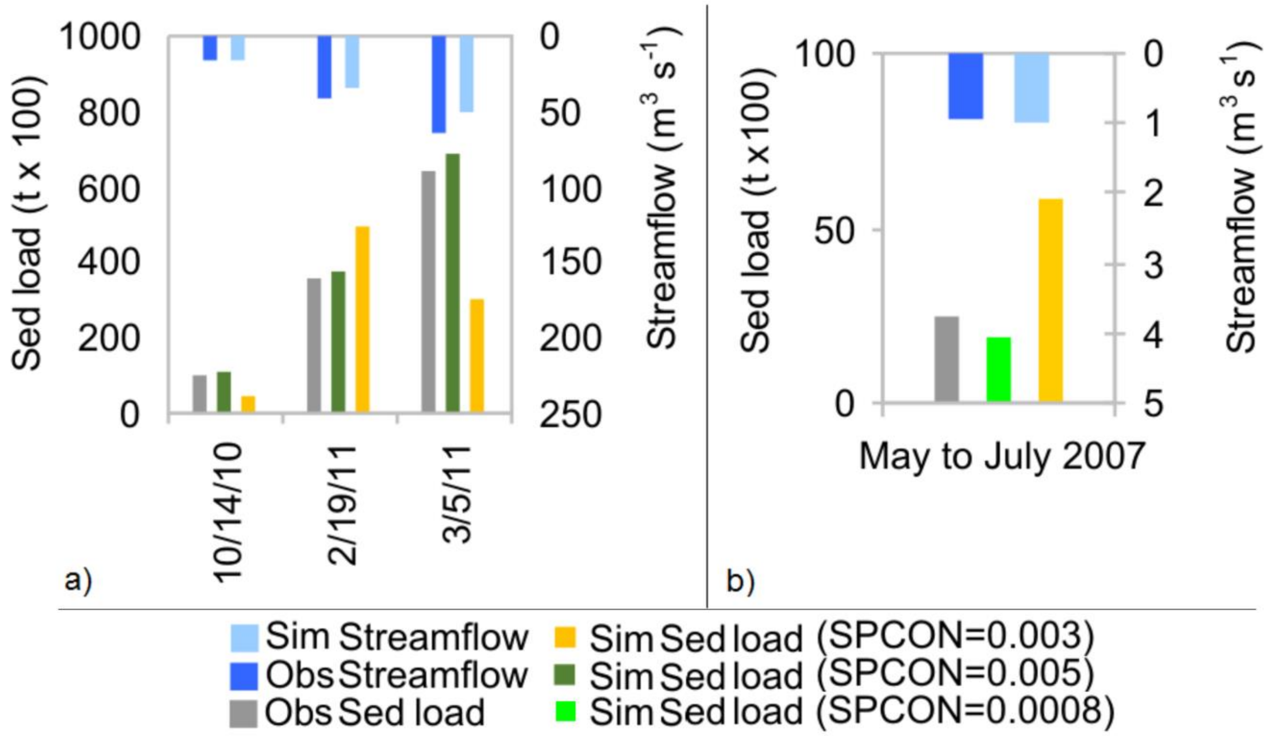

Figure 5. a) Observed and simulated streamflow for three events; observed and simulated sediment load from the whole hydrological year value (SPCON = 0.003) and seasonal calibration value for channel routing (SPCON = 0.005). b) Observed and simulated streamflow for three months, observed and simulated sediment load from the whole hydrological year value (SPCON = 0.003) and seasonal calibration value for channel routing (SPCON = 0.0008).

3.2 Streamflow and sediment load

Analysis of the model results for the five-year study period on a basin scale show that only 17% of rainfall (119 mm of the average yearly value of 686 mm) reaches the river network through surface runoff, and 85% (500 mm) is lost via evapotranspiration, which is a value similar to those obtained from other studies in the same region (Romanazzi *et al*., 2015). A total water yield, considered as the sum of surface runoff, lateral flow, and groundwater contribution net of transmission losses, of 186 mm was simulated, corresponding to 27% of the total rainfall, while the average annual sediment loading was 6.8 t ha^{-1} yr^{-1}.

The pattern of sediment load at the outlet of the watershed follows the pattern of streamflow (Figure 6). Sediment dynamics in the Carapelle watershed show a winter (December to April) dominant erosion pattern, caused by rainfall events. At the outlet, about 60% of the average annual discharge, and nearly 90% of the annual sediment load, are transported in the wet season (October to April). Meanwhile, during the dry months (May to September), sediment loading is very low ($\leq$ 0.2 t ha^{-1}). High inter-annual variability was simulated in sediment loads, ranging from 3.18 t ha^{-1} yr^{-1} to 12.1 t ha^{-1} yr^{-1}, as a consequence of different climatic conditions recorded in 2008 and 2009, with yearly rainfalls of 553 mm and 829 mm, respectively.

The hillslope sediment delivery ratio (SDR) was computed for the whole basin as the ratio of sediment yield to the stream at the outlet, divided by the gross erosion occurring on the hillslopes. SDR is generally interpreted as transport efficiency of sediment from the hillslopes to the stream network (Ferro & Porto 2000; Lu *et al*., 2006). In the study area, the average annual SDR assumes a value of 0.3, ranging from 0.19 to 0.42 for the driest and wettest years, 2008 and 2009, respectively.

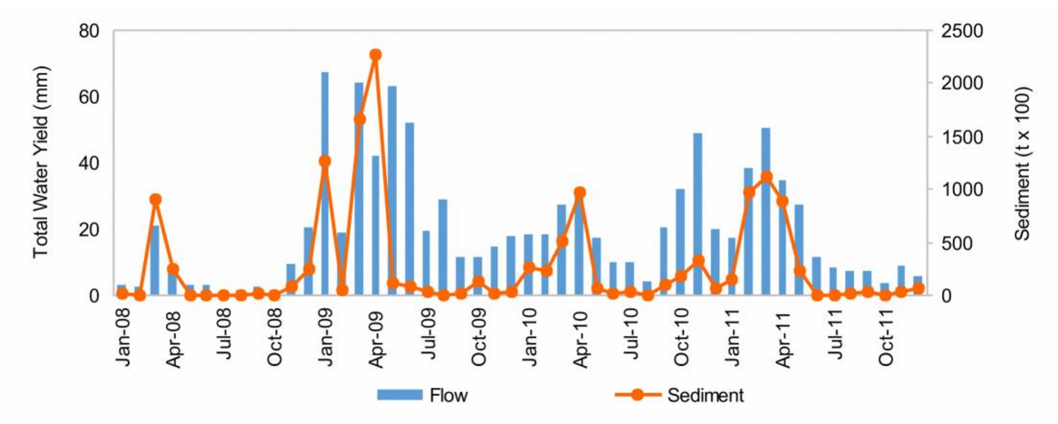

Figure 6. Comparison between streamflow and sediment load.

3.3 Sediment source areas

Analysing the model results on a sub-basin scale, a high difference in soil loss among the upper, central, and lower parts of the study area can be observed (Figure 7a). The upstream area is characterised by high erosion rates (7-13 t ha^{-1} yr^{-1}), which slowly decrease along the downstream sub-basins. The morphology has a great influence on erosion. Indeed, sub-basins showing the highest annual erosion (e.g. sub-basins 16, 17) are characterised by steep slopes, while low values of soil loss (<1 t ha^{-1} yr^{-1}) are simulated in the flat sub-basins (e.g. sub-basins 1, 2, and 3).

Figure 7b shows, with respect to deposition in the reaches, the highest value, simulated in the central part of the Carapelle basin, which is downstream of the steeper reaches, where there is a first alluvial plain (sub-basin 15). Here, the river assumes a braided course, and there is deposition of the coarser material. The mountainous part of the basin shows an absence of, or very low, deposition (<0.15 t ha^{-1} yr^{-1}).

Furthermore, the principal land uses, as identified by the model in the HRU analysis, as well as the rainfall, slope, and soil types, were related to the sediment yield in order to identify the main source areas (Table IV). The result of this analysis evidences that the mean annual specific sediment loss is mostly conditioned by rainfall and slope. For instance, the model simulates a sediment loss for winter wheat ranging from 0.1 t ha^{-1} yr^{-1} to 15 t ha^{-1} yr^{-1}. It seems that soil texture exerts a minor influence, especially in the upper part of the basin. This is due to the fact that soils, classified as clay and clay-loam in the mountainous part of the basin, show similar properties. The highest value of soil loss is predicted for the winter wheat crop, with a sediment loss of 15.38 t ha^{-1} yr^{-1}, under average annual rainfall of about 900 mm, along a steep slope (15%). As expected, forest and rangeland show lower values of sediment loss.

Figure 7c, which is colour-coded by land use, shows all the critical HRUs in the sub-basins that are characterised by a mean annual sediment yield greater than the threshold value of 1.40 t ha^{-1} y^{-1} set by Verheijen *et al*. (2009). This threshold value represents tolerable soil erosion for conditions prevalent in Europe, for which a deterioration or loss of one or more soil functions does not occur. In the same figure, the white HRUs are characterised by tolerable erosion values.

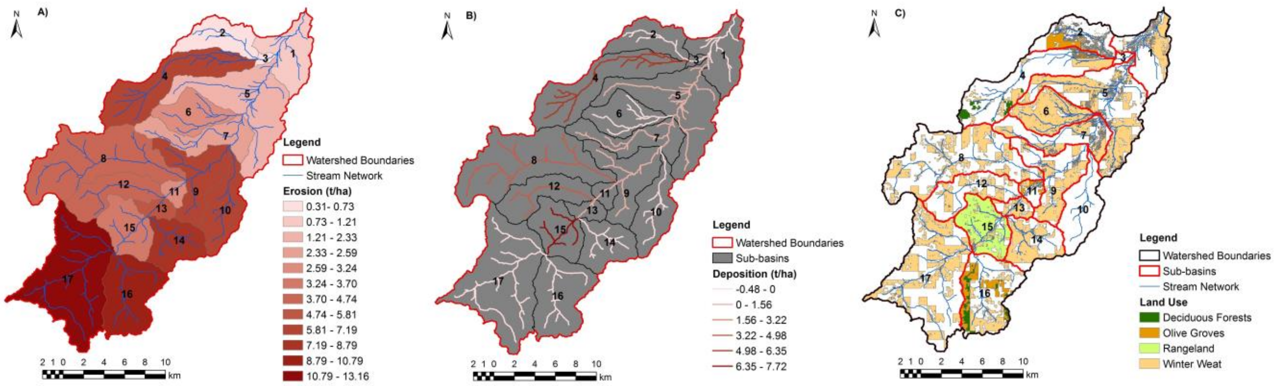

Figure 7. a) Average annual sediment yield on sub-basin scale; b) average annual sediment deposition in channel; c) location of critical HRUs in sub-basins as a function of land use.

Table IV. Mean annual sediment yield for each sub-basin as a function of land use, rainfall, soil type, and slope.

Subbasins	Land use	Rainfall (mm)	Soil type	Slope (%) min	Slope (%) max	Sediment Yield (t ha-1 yr-1) min	Sediment Yield (t ha-1 yr-1) max
1	Winter wheat	578.68	Silty-Clay-Loam/Clay-Loam	0.23	7.18	0.05	1.67
	Olive Groves	578.68	Silty-Clay-Loam/Clay-Loam	8.38	9.20	2.07	2.34
2	Winter wheat	612.28	Silty-Clay/Clay-Loam	0.28	6.45	0.08	1.41
3	Winter wheat	578.68	Silty-Clay-Loam/Clay-Loam	0.25	6.36	0.05	1.06
4	Deciduous Forests	847.4	Clay/Clay-Loam	25.08	27.05	1.7	7.49
	Winter wheat	847.4	Silty-Clay/Silty-Clay-Loam/Clay-Loam	0.25	15.07	0.26	13.83
	Olive Groves	847.4	Clay-Loam	15.04		8.22	
5	Winter wheat	578.68	Silty-Clay/Clay-Loam	4.52	9.48	0.72	2.77
6	Winter wheat	592.84	Clay/Silty-Clay	11.49	11.89	3.08	3.36
7	Winter wheat	578.68	Clay/Silty-Clay/Clay-Loam	7.94	11.40	1.98	3.45
8	Rangeland	592.84	Clay/Clay-Loam	26.85	30.85	0.36	0.79
	Deciduous Forests	592.84	Clay-Loam	28.90		0.11	
	Winter wheat	592.84	Clay/Clay-Loam	16.65	17.46	5.76	6.76
9	Winter wheat	702.8	Clay/Silty-Clay/Clay-Loam	10.19	16.25	5.33	10.61
10	Winter wheat	702.8	Clay/Clay-Loam	12.78	14.41	6.59	8.59
	Deciduous Forests	702.8	Clay/Clay-Loam	19.10	23.97	0.22	0.68
11	Winter wheat	702.8	Silty-Clay-Loam/Clay-Loam	0.14	15.61	0.13	8.75
	Rangeland	702.8	Clay-Loam	18.49		0.25	
	Deciduous Forests	702.8	Clay-Loam	21.62		0.25	
	Beushes and srhubs	702.8	Clay-Loam	0.12	19.76	0.13	0.16
12	Winter wheat	592.84	Clay/Clay-Loam	13.30	16.75	3.52	6.27
	Deciduous Forests	592.84	Clay-Loam	33.40		0.13	
	Beushes and srhubs	592.84	Clay/Clay-Loam	25.87	26.45	0.07	0.25
	Olive Groves	592.84	Clay/Clay-Loam	23.82	26.36	3.21	3.42
13	Deciduous Forests	702.8	Clay-Loam	23.11		0.27	
	Beushes and srhubs	702.8	Clay-Loam	22.49		0.17	
	Winter wheat	702.8	Clay/Clay-Loam	12.64	16.31	5.58	10.3
14	Rangeland	702.8	Clay/Clay-Loam	18.27	18.45	0.25	0.34
	Winter wheat	702.8	Clay/Clay-Loam	15.08	15.22	9.68	9.74
15	Rangeland	592.84	Clay/Clay-Loam	14.60	19.25	0.13	0.3
	Winter wheat	592.84	Clay/Clay-Loam	13.21	14.26	4.19	4.28

	Rangeland	719.08	Clay/Clay-Loam	21.65	23.00	8.02	13.63
16	Deciduous Forests	719.08	Clay-Loam	23.87		1.41	
	Winter wheat	719.08	Clay/Clay-Loam	16.92	18.59	10.67	13.99
	Olive Groves	719.08	Clay-Loam	19.37		12.64	
17	Rangeland	898.88	Clay/Clay-Loam	18.53	20.22	0.57	0.64
	Winter wheat	898.88	Clay/Clay-Loam	14.14	15.08	13.23	15.38

4. Discussion

4.1 Modelling streamflow

The results obtained reveal that the SWAT model is able to predict runoff in the Carapelle basin, despite the complexity of the catchment area and limited availability of input data. The automatic procedures (SUFI-2 in SWAT-CUP) used to calibrate the hydrological processes proved to be successful assistance tools, despite the numerous parameters that should be taken into account.

It has been found that the most sensitive hydrological parameters are closely related to evapotranspiration (i.e. soil evaporation compensation factor) and surface runoff processes (i.e. curve number). Hence, it can be stated that the streamflow regime in the Carapelle basin is dominated by surface runoff, while the baseflow has a minor influence on total water yield. Our study confirms the results of similar studies in southern Italy (De Girolamo *et al*., 2017, Licciardello *et al*., 2017).

Streamflow simulation performances, analysed with statistical indices (R^2, NSE, PBIAS) on a daily time interval, showed better results for the calibration period, compared to the validation period where only the PBIAS value can be considered very good, while the R^2 and NSE values are unsatisfactory; however, when analysing the obtained results on a monthly scale, and using the performance thresholds suggested by Moriasi *et al*., (2007), SWAT showed a satisfactory performance in simulating streamflow. These results are in agreement with several studies, which reported that model simulations are poorer using daily time intervals, with respect to monthly or yearly ones (Fernandez *et al*., 2005; Grizzetti *et al*., 2005; Engel *et al*., 2007; De Girolamo *et al*., 2015).

To better understand the performance of the model, a more detailed analysis was performed, in order to have information about which periods are simulated with greater or lesser success. What emerged from this analysis is that the SWAT model tends to better predict streamflow in the wet season, compared to the dry season. In particular, streamflow is generally over-predicted in the dry season. This statement is also confirmed by several studies that have reported a discrepancy between observed and simulated streamflow in extremely low flow conditions (Muleta *et al*., 2012). Guse *et al*. (2013) identified groundwater and evapotranspiration parameters as the main reasons for the low performance in the dry season. Moreover, it is well known that temporary rivers are one of the most unstable river systems, and among the most intensively endangered by hydrological fluctuations (Larned *et al*., 2010). For these watersheds, the capacity of hydrological models in simulating extremely low flow conditions has been discussed (Kirkby *et al*., 2011; De Girolamo *et al*., 2015).

It should be also considered that the reliability of the data, especially that for rainfall, used in the model simulations plays a relevant role in model results. A lack of direct correspondence between rainfall and observed streamflow was found both in the calibration and in the validation periods. In particular, some peaks of flow were recorded in the absence of measured rainfall events. This discrepancy can be due to errors in measurements (rainfall or streamflow), or to convective rainfall events localised in small areas around the stations, or gaps in the time-series. In addition, the number of gauging stations and their locations, which in our study were not spatially well-distributed across the basin, can have a great influence on model performance. Moreover, we have verified the presence of missing data in rainfall data series. To fill the gaps, we used the weather generator module, included in the SWAT model, which estimates the missing data through equations based on weather parameter statistics of the monitoring stations. However, although the method works well in filling the gaps, it is expected that the estimated rainfall could be different from the true values and, consequently, simulated peak flows may not match measured values. A large number of statistical techniques is available to fill the gaps in rainfall time-series (Barca *et al*., 2016). For the Mediterranean climate, a more reliable method for filling the gaps than that used by the SWAT model could be the 'weighted similarity index', which is based on the similarity of some factors between stations (geomorphological and statistical correlation). These methods require time-series of climatic data recorded at several gauging stations, both inside and outside the basin, which were not available for our study.

According to Strauch *et al*. (2012), another method to enhance SWAT simulation results is to use radar data precipitation, while, White *et al*. (2009) used the seasonal calibration scheme. The best strategy should be selected case by case after a critical analysis of the study area and the simulation results. In this study, radar data are not available and the discrepancies between simulated and observed streamflow in the dry period were mainly due to few events caused by convective rainfall, therefore a seasonal calibration scheme for streamflow was not carried out.

4.2 Modeling sediment load

Generally, the SWAT model has proven to simulate runoff better than sediment load. The range of values obtained in sediment calibration and validation is nevertheless satisfactory (Moriasi *et al*., 2007) and similar to those reported by Zabaleta *et al*. (2014), Beeson *et al*. (2014), and Almendinger *et al*. (2014). There may be different reasons for low model performance in simulating sediment load. Many authors have complained about problems related to measured sediment data, such as the need for a large record to test the model profoundly (Bonumá *et al*., 2014), deficiency of data authenticity (Bieger *et al*., 2014), and poor statistical accuracy, due to the small magnitude of sediment load (Lu *et al*., 2014). In this study, as already reported by Bieger *et al*. (2014), the coarse resolution of DEM, soil and land use data, in addition to problems in the transferability of the MUSLE approach (Williams & Berndt, 1977) could be a reason for poor sediment yield simulation. Moreover, the SWAT model does not simulate bank erosion (Abouabdillah *et al*., 2014), which is an active process in the study area. On the other hand, point sources of sediment (i.e. mass movements) and connectivity remain difficult to describe in most models (De Vente *et al*., 2006). Indeed, several landslides have been enumerated, caused by the geotechnical properties of the units present in the area (clay-flysch). The activity of landslides is characterised by remobilisation of slope movement, related to rainfall events, which are the most relevant triggers of landslides (Wasowski *et al*., 2007). It should be kept in mind that, besides all previously given reasons that could lead to model inefficiency, especially in semi-arid zones (Douglas-Mankin *et al*., 2010), hydrological models experience prediction uncertainty due to their own structure, input data, and parameters (Refsgaard *et al*., 2007).

For sediments, the most sensitive parameter is the peak rate adjustment factor (ADJ_PKR) for sediment routing in the sub-basin. This result is expected, as most of the sediment load is transported during floods. Additionally, the linear parameter for calculating the maximum amount of sediment that can be re-entrained during channel sediment routing (SPCON) was also found to be sensitive. In the seasonal calibration, a combination of two different values for this parameter, for the dry (0.0008) and wet periods (0.005), was found and implemented in order to improve channel sediment routing in the Carapelle river system. This is because, when the multiplication coefficient of the peak channel velocity in the Bagnold equation (SPCON) assumes a high value, the maximum transport capacity (i.e. concentration limit) increases. At the beginning of each time interval, the SWAT compares the inflow sediment concentration to the concentration limit. If the inflow concentration exceeds the limit, deposition occurs until a maximum sediment concentration is reached. The seasonal calibration can be justified for use in the dry season because the river network is a continuum where completely dry river segments and perennial reaches coexist, and flow conditions are very dissimilar from those of the wet period (De Girolamo *et al*., 2017). On the other hand, the results show that, with this approach, simulated and observed sediment loads are in very good agreement for flood events and for the dry period. Hence, we can say that it is necessary to go beyond statistical performance and select the best set of parameters, taking into account the processes acting in the basin and the final objectives of the work. In this case, expert knowledge can be fundamental in making the conceptual model more realistic. Finally, our results show that the daily timescale adopted in this study is relevant for studying streamflow and sediment load regimes when the duration of flood events is a few days (or hours), as in the Carapelle basin, where the average monthly values were potentially not representative. The seasonal calibration scheme has already been used in SWAT for runoff (Lèvesque *et al*., 2008; Guse *et al*., 2013; Zangh *et al*., 2015), and our results verify that this approach can be used also for improving the performance of sediment simulation.

4.3 Sediment source areas

On a basin scale, the SWAT model simulated an average sediment yield of 6.8 t ha^{-1} yr^{-1}. These results are in line with those presented by Van Rompaey *et al*. (2005) for watersheds with similar characteristics in southern Italy; however, a large difference was found within the basin with regard to soil loss, ranging from 0 to 15 t ha^{-1} yr^{-1}. This estimation is higher than what was reported for the northern areas of the Apulia region by Panagos *et al*. (2015), who found erosion rates ranging from 5 to 10 t ha^{-1} yr^{-1} by applying the RUSLE equation. It has been speculated that this difference is due to the different data resolution used in these two studies.

Through analysis of soil loss on the sub-basin scale, a gradient was identified between the highest values in the mountainous part of the basin (subs 16 and 17) and the lowest values in flat areas (subs 1, 2, and 3). As an important role in soil erosion is played by the slope (Licciardello *et al*., 2017), upstream sub-basins are characterised by higher values of slope, compared to the downstream areas. Slope can also be considered a key factor in the case of deposition, such that higher values are concentrated in the central part of the watershed, where the slope is lower than the upstream area.

Based on this analysis, there are some sub-basins that apparently show anomalous results, such as 4 and 15. The former has both high erosion and deposition rates, as it is characterised by an upstream area with a high slope and flat downstream area. As a result, most of the sediment generated upstream is deposited in the same reach. On the other hand, sub-basin 15, although being located in the upstream area of the watershed, is also located downstream of the steeper reaches, and is characterised by an alluvial plain. For this reason, it has high deposition and medium erosion rates.

It is known that low-slope areas limit sediment transport connection, in contrast to how an increase in the slope improves the connectivity (Borselli *et al*., 2008). It can, therefore, be stated that the Carapelle watershed has a middle area, where reaches receive and store many sediments, which causes a poor connectivity between the upstream area and the outlet. Generally, comparison between erosion and deposition maps reveals that SWAT is able to determine the sediment source locations, both in sub-basins and HRUs (Figure 7), as well as in the sink zones located in reaches. Moreover, the SWAT model, once efficiently calibrated and validated, can be used in scenario analysis to assess connectivity modifications in sediment migration modelling due to land use changes (Le Roux *et al*., 2013).

Soil formation rates are generally very low. For example, 100 to 400 years are needed to develop one centimetre of topsoil in Europe. Verheijen *et al*. (2009) found a rate of soil formation of 1.40 t ha^{-1} y^{-1} (0.056 mm yr^{-1}). This study show that land degradation in the Carapelle basin is a problem, indeed the soil loss (~7 t ha^{-1} yr^{-1}, corresponding to 0.24 mm yr^{-1}) is higher than this value. This means that soil is being lost much faster than the rate of renewal, and that soil erosion is effectively irreversible, with potentially high environmental and economic impacts.

At the level of HRUs, land cover is a very significant factor (Licciardello *et al*., 2017), in addition to slope and precipitation, required to determine which areas have a high risk of erosion within sub-basins. The map in Figure 7c and Table IV show that, in the Carapelle watershed, winter wheat and olive groves are the major source areas. As expected, forest and rangeland represent the land use producing the lowest soil losses for each class of soil and slope. There are only a few forest and rangeland areas that produce sediment higher than the indicated threshold (i.e. > 1.40 t ha^{-1} y^{-1}). Winter wheat (76% of the total area) requires tillage in autumn, leaving soils unprotected for most of the wet season (Trombetta *et al*., 2016). Additionally, erosion is facilitated by deep, and up and down, ploughing, which is quite common in this basin. In order to correctly reproduce the deep and up and down ploughing, the SWAT2012.mdb database was modified, substituting the default value of depth of plough (moldboard plough 2 way) with a new one (400 mm). Moreover, high values of CN (from 82 to 87) were used to simulate the unprotected soil conditions. Indeed, to take into account the presence of vegetation in forests and rangeland areas, low values of CN were used (from 65 to 72). Rainfall characteristics and soil type (mainly clay-loam), contributed to the erosion, as well as landslide activities. Hence, the combined analysis of Figure 7 and Table IV is very significant for determining the sources of sediments and their locations within sub-basins. Moreover, they are useful instruments in helping to prioritise the implementation of BMPs in the watersheds (Betrie *et al*., 2011).

This study confirms that Mediterranean watersheds are fragile agro-ecosystems because soil essentially constitutes a non-renewable resource (López-Vicente *et al*., 2013). Hence, to mitigate the impact of agriculture on soil depletion, BMPs have to be considered by the policy-makers of regional, national, and European Union institutions. A combination of agricultural (e.g. direct sowing of wheat with no tillage operation) and environmental measures (e.g. reforestation of the riparian buffers) may reduce soil erosion from the watershed (Abdelwahab *et al*., 2014). For this purpose, analysis of sediment source zones and deposition areas is crucial, as shown by Dickinson *et al*. (1990), who reported that there is an economic advantage to identifying the areas that have a higher potential to deliver sediment, with the aim of prioritising the implementation of control measures, and to facilitate planning for sustainable land management.

Conclusions

This study reports the results of the SWAT model application in simulating streamflow and sediment yield, and identifying sediment source areas in the Carapelle watershed. We intend this to be a contribution to help improve techniques for calibrating hydrology and sediment load in watersheds under Mediterranean climates, where the high variability of rainfall and hydrological regime makes it difficult to reproduce low flow and sediment accurately. The results of the present work show that the SWAT model is able to assess hydrological and sediment. On the other hand, the study confirms the problems associated with characterising the complexity and range of the environmental variables of these basins, as already reported in the literature. The automatic procedure used for calibrating the hydrological processes proved to be a successful assistance tool; however, it generally over-predicts streamflow in the dry season. The model tends to better predict streamflow in the wet season, and it has proven to simulate runoff better than sediment load. The statistical performance in a global calibration of sediment load, on a monthly timescale, is satisfactory; however, on a daily timescale, the results are unsatisfactory for the validation period. Hence, to further improve sediment performance here, a combination of two different values of the Bagnold's equation parameter were proposed for the channel sediment routing, for the wet and dry seasons, respectively. With this strategy, the performance of the model is acceptable for both wet and dry periods, also on a daily timescale, and major flood events are well predicted for streamflow and sediment load. In the study area, the results show that erosion was mainly a winter process, and the major sources of sediment are those sub-basins characterised by steep slopes, where sediment mainly originates from winter wheat fields. The results also show that soil is being lost faster than the rate of replenishment, and that the soil erosion process is irreversible in the Carapelle basin. To mitigate the impact of agriculture on soil depletion and land degradation, conservative agricultural practices, and positive environmental measures have to be considered by policy-makers. For this purpose, the SWAT model is a useful tool because it permits the identification of areas that are at high risk of erosion and where different management options can be implemented for sustainable land management.

Acknowledgements

This research was conducted in the framework of the COST action ES1306 “Connecteur”: Connecting European Connectivity Research (chair Saskia Keesstra, Wageningen University) as an outcome of the Meeting “Hydrological and Erosion processes in Mediterranean Landscapes: Impacts of land management on connectivity” held in Palermo, February 28- March 5, 2016.

References

Abbaspour KC, Rouholahnejad E, Vaghefi S, Srinivasan R, Yang H, & Kløve B. 2015. A continental-scale hydrology and water quality model for Europe: Calibration and uncertainty of a high-resolution large-scale SWAT model. *Journal of Hydrology*, **524**: 733-752 DOI: http://dx.doi.org/10.1016/j.jhydrol.2015.03.027

Abbaspour KC, Yang J, Maximov I, Siber R, Bogner K, Mieleitner J, Srinivasan R. 2007. Modelling hydrology and water quality in the pre-alpine/alpine Thur watershed using SWAT. *Journal of Hydrology*, **333** (2–4): 413-430. DOI: http://dx.doi.org/10.1016/j.jhydrol.2006.09.014

Abdelwahab OMM, Bingner RL, Milillo F, & Gentile, F. 2014. Effectiveness of alternative management scenarios on the sediment load in a Mediterranean agricultural watershed. *Journal of Agricultural Engineering*, **45**(3): 125-136.

Abdelwahab OMM, Bingner RL, Milillo F, & Gentile F. 2016. Evaluation of Alternative Management Practices With the AnnAGNPS Model in the Carapelle Watershed. *Soil Science*, **181**(7):, 293-305. DOI: 10.1097/ss.0000000000000162

Abdelwahab OMM, Bisantino T, Milillo F, Gentile F. 2013. Runoff and sediment yield modeling in a medium-size mediterranean watershed. *Journal of Agricultural Engineering*, **44**: 31-40. DOI: 10.4081/jae.2013.(s1):e7

Abouabdillah A, White M, Arnold JG, De Girolamo AM, Oueslati O, Maataoui A, & Lo Porto A. 2014. Evaluation of soil and water conservation measures in a semi-arid river basin in Tunisia using SWAT. *Soil Use and Management*, **30**(4): 539-549. DOI: 10.1111/sum.12146.

Almendinger JE, Murphy MS, & Ulrich JS. 2014. Use of the Soil and Water Assessment Tool to Scale Sediment Delivery from Field to Watershed in an Agricultural Landscape with Topographic Depressions. *Journal of Environmental Quality*, ***43***(1):, 9-17. DOI: 10.2134/jeq2011.0340.

Arnold JG, Engel BA, Srinivasan R. 1993. A continuous time, grid cell watershed model. Proceedings of the application of advanced information tecnologies: effecctive management of natural resource conference. *ASAE*, St. Joseph, MI.

Arnold JG, Moriasi DN, Gassman PW, Abbaspour KC, White MJ, Srinivasan R, Jha MK. 2012. Swat: Model use, Calibration, and Validation. *Transactions of the ASABE*, **55**(4): 1491-1508

Arnold JG, Srinivasan R, Muttiah RS, & Williams JR 1998. Large area hydrologic modeling and assessment - Part 1: Model development. *Journal of the American Water Resources Association*, **34**(1): 73-89. DOI: 10.1111/j.1752-1688.1998.tb05961.x

Asres MT & Awulachew SB. 2010. SWAT based runoff and sediment yield modelling: a case study of the Gumera watershed in the Blue Nile basin. *Ecohydrology & Hydrobiology*, **10**(2–4): 191-199. DOI: http://dx.doi.org/10.2478/v10104-011-0020-9

Bagnold RA. 1977. Bed load transport by natural rivers. *Water Resources Research*, **13**(2): 303-312. DOI: 10.1029/WR013i002p00303

Ballabio C, Panagos P, & Monatanarella L. 2016. Mapping topsoil physical properties at European scale using the LUCAS database. *Geoderma*, **261**: 110-123. DOI: http://dx.doi.org/10.1016/j.geoderma.2015.07.006

Barca E, Bruno DE, Passarella G. 2016. Similarity indices of meteo-climatic gauging stations: definition and comparison. Environmental Monitoring and Assessment **188**(7), 1-12

Beeson PC, Sadeghi AM, Lang MW, Tomer MD, & Daughtry CST. 2014. Sediment Delivery Estimates in Water Quality Models Altered by Resolution and Source of Topographic Data. *Journal of Environmental Quality*, **43**(1): 26-36. DOI: 10.2134/jeq2012.0148

Betrie GD, Mohamed YA, Griensven A, Srinivasan R. 2011. Sediment management modelling in the Blue Nile Basin using SWAT model. *Hydrology and Earth System Sciences*, **15**: 807-818. DOI: 10.5194/hess-15-807-2011

Bieger K, Hormann G, & Fohrer N. 2014. Simulation of Streamflow and Sediment with the Soil and Water Assessment Tool in a Data Scarce Catchment in the Three Gorges Region, China. *Journal of Environmental Quality*, **43**(1): 37-45. DOI: 10.2134/jeq2011.0383

Bingner RL & Theurer FD. 2005. AnnAGNPS technical processes documentation,version 3.2. Oxford, MS, USA: USDA-ARS National Sedimentation Laboratory

Bisantino T, Bingner R, Chouaib W, Gentile F, & Trisorio Liuzzi G. 2015. Estimation of runoff, peak discharge and sediment load at the event scale in a medium-size mediterranean watershed using the AnnAGNPS model. *Land Degradation & Development*, **26**(4): 340-355. DOI: 10.1002/ldr.2213

Bisantino T, Gentile F, Milella P, Trisorio Liuzzi G. 2010. Effect of time scale on the performance of different sediment transport formulas in a semiarid region *Journal of Hydraulic Engineering*, **136** (1): 56-61. DOI: 10.1061/(ASCE)HY.1943-7900.0000125

Bonumà NB, Rossi CG, Arnold JG, Reichert JM, Minella JP, Allen PM, & Volk M. 2014. Simulating Landscape Sediment Transport Capacity by Using a Modified SWAT Model. *Journal of Environmental Quality*, **43**(1): 55-66. DOI: 10.2134/jeq2012.0217

Borselli L, Cassi P, Torri D. 2008. Prolegomena to sediment and flow connectivity in the landscape: A GIS and field numerical assessment. *Catena*, **75:** 268-277.

Briak H, Moussadek R, Aboumaria K, Mrabet R. 2016. Assessing sediment yield in Kalaya gauged watershed (Northern Morocco) using GIS and SWAT model. *Internationa Soil and Water Conservation Research*, **4**; 177-185. DOI; https://doi.org/10.1016/j.iswcr.2016.08.002

Cerdà A, Lavee H, Romero-Díaz A, Hooke J, & Montanarella L. 2010. Preface:Soil erosion and degradation in Mediterranean type ecosystems *Land Degradation & Development*, **21**(2): 71-74. DOI: 10.1002/ldr.968

Chen H, Luo Y, Potter C, Moran PJ, Grieneisen ML, Zhang M. 2017. Modeling pesticide diuron from the San Joaquin watershed into the Sacramento-San Joaquin Delta using SWAT. *Water Research*. DOI: http://dx.doi.org/10.1016/j.watres.2017.05.032

Collins AL & Walling DE. 2004. Documenting catchment suspended sediment sources: problems, approaches and prospects. *Progress in Physical Geography*, **28**(2): 159-196. DOI:10.1191/0309133304pp409ra

De Girolamo AM, Barca E, Pappagallo G, & Lo Porto A. 2017. Simulating ecologically relevant hydrological indicators in a temporary river system. *Agricultural Water Management*, **180** part B: 194-204. DOI: http://dx.doi.org/10.1016/j.agwat.2016.05.034

De Girolamo AM, Lo Porto A, Pappagallo G, Tzoraki O, & Gallart F. 2015. The Hydrological Status Concept: Application at a Temporary River (Candelaro, Italy). *River Research and Applications*, **31**(7): 892-903. DOI: 10.1002/rra.2786

Douglas-Mankin KR, Srinivasan R, & Arnold JG. 2010. Soil and Water Assessment Tool (SWAT) Model: Current Developments and Applications. **53**(5). DOI: 10.13031/2013.34915

Dickinson WT, Wall GJ, & Rudra RP. 1990. Model-building for predicting and managing soil-erosion and transport. *Chichester: John Wiley & Sons Ltd*

Di Stefano C & Ferro V. 2017. Testing sediment connectivity at the experimental SPA2 basin,Sicily (Italy). *Land Degradation & Development.* DOI: 10.1002/ldr.2722

EAWAG. 2013. SWAT-CUP 2012: SWAT Calibration and Uncertainty Programs - A User Manual. *Swiss Federal Institute of Aquatic Science and Technology, Switzerland*

EC. 2006. Commission staff working document “Impact Assessment of the Thematic Strategy on Soil Protection” (SEC(2006)620) Avaliable online: http://eur-lex.europa.eu/legal-content/EN/TXT/?uri=CELEX:52006PC0232 (accessed on 15 December 2016)

Engel B, Storm D, White M, Arnold JG, & Arabi M. 2007. A hydrologic/water quality model application protocol. *Journal of the American Water Resources Association*, **43**(5): 1223-1236. DOI: 10.1111/j.1752-1688.2007.00105.x.

Fernandez GP, Chescheir GM, Skaggs RW, & Amatya DM. 2005. Development and testing of watershed-scale models for poorly drained soils. *Transactions of the ASAE*, **48**(2): 639-652.

Ferro V & Porto P. 2000. Sediment delivery distributed (SEDD) model. *Journal of Hydrologic Engineering*, **5**(4): 411-422. DOI: 10.1061/(asce)1084-0699(2000)5:4(411)

Flanagan DC, Frankenberger JR, & Ascough JC, II. 2012. WEPP: model use, calibration, and validation. *Transactions of the ASABE*, **55**(4): 1463-1477

Fryirs KA, Brierley GJ, Preston, NJ, & Kasai M. 2007. Buffers, barriers and blankets: The (dis)connectivity of catchment-scale sediment cascades. *Catena*, **70**(1): 49-67. DOI: 10.1016/j.catena.2006.07.007

Furl C, Sharif H, Jeong J. 2015. Analysis and simulation of large erosion events at central Texas unit source watersheds. *Journal of Hydrology*, **527**; 494-504. DOI: http://dx.doi.org/10.1016/j.jhydrol.2015.05.014

Gamvroudis C, Nikolaidis NP, Tzoraki O, Papadoulakis V, & Karalemas N. 2015. Water and sediment transport modeling of a large temporary river basin in Greece. *Science of The Total Environment*, **508**: 354-365. DOI: http://dx.doi.org/10.1016/j.scitotenv.2014.12.005

Gan TY, Dlamini EM, & Biftu GF. 1997. Effects of model complexity and structure, data quality, and objective functions on hydrologic modeling. *Journal of Hydrology*, **192**(1-4): 81-103

García-Ruiz JM, Beguería S, Lana-Renault N, Nadal-Romero E, & Cerdà A. 2016. Ongoing and Emerging Questions in Water Erosion Studies. *Land Degradation & Development*, DOI: 10.1002/ldr.2641

García-Rama, A, Pagano, SG, Gentile, F, Lenzi, MA (2016) Suspended sediment transport analysis in two Italian instrumented catchments. *Journal of Mountain Science*, 13 (6), 957-970. DOI: 10.1007/s11629-016-3858-x

Gassman PW, Williams JR, Wang X, Saleh A, Osei E, Hauck LM, Flowers JD. 2010. The agricultural policy/environmental extender (APEX) model: an emerging tool for landscape and watershed environmental analyses. *Transactions of the ASABE*, **53**(3): 711-740

Gentile F, Bisantino T, Corbino R, Milillo F, Romano G, Trisorio Liuzzi G. 2010. Monitoring and analysis of suspended sediment transport dynamics in the Carapelle torrent (Southern Italy) *Catena*, **80**(1): 1-8. DOI: 10.1016/j.catena.2009.08.004

Glavan M, Pintar M, Volk M, 2013. Land Use change in a 200-year period and its effect on blue and green water flow in two Slovenian Mediterranean catchments-lessons for the future. Hydrol. Process. **27**: 3964–3980. DOI: 10.1002/hyp.9540

Gyamfi C, Ndambuki JM, Salim RW. 2016. Simulation of Sediment Yield in a Semi-Arid River Basin under Changing Land Use: An Integrated Approach of Hydrologic Modelling and Principal Component Analysis. *Sustainability*.

Götzinger J & Bárdossy A. 2008. Generic error model for calibration and uncertainty estimation of hydrological models. *Water Resources Research*, **44**(12). DOI: 10.1029/2007WR006691

Grizzetti B, Bouraoui F, de Marsily G, & Bidoglio G. 2005. A statistical method for source apportionment of riverine nitrogen loads. *Journal of Hydrology*, **304**(1-4): 302-315. DOI: 10.1016/j.jhydrol.2004.07.036

Gupta H, Sorooshian S, & Yapo P. 1999. Status of Automatic Calibration for Hydrologic Models: Comparison with Multilevel Expert Calibration. *Journal of Hydrologic Engineering*, **4**(2): 135-143. DOI:10.1061/(ASCE)1084-0699(1999)4:2(135)

Guse B, Reusser DE, & Fohrer N. 2013. How to improve the representation of hydrological processes in SWAT for a lowland catchment - temporal analysis of parameter sensitivity and model performance. *Hydrological Processes*, **28**(4): 2651-2670. DOI: 10.1002/hyp.9777

Hargreaves GH. 1975. Moisture Availability and Crop Production. *Transactions of the ASAE*, **18**(5): 980-984. DOI: 10.13031/2013.36722

Hiederer R, Jones RJA, & Daroussin J. 2006. Soil Profile Analytical Database for Europe (SPADE): Reconstruction and validation of the measured data (SPADE/M). *Geografisk Tidsskrift*, **106**(1): 71-85

Hooke J. 2003. Coarse sediment connectivity in river channel systems: a conceptual framework and methodology. *Geomorphology*, **56**: 79-94

Jones DL, Rousk J, Edwards-Jones G, DeLuca TH, & Murphy DV. 2012. Biochar-mediated changes in soil quality and plant growth in a three year field trial. *Soil Biology & Biochemistry*, **45**: 113-124. DOI: 10.1016/j.soilbio.2011.10.012

Kalin L & Hantush MM. 2006. Hydrologic modeling of an eastern Pennsylvania watershed with NEXRAD and rain gauge data. *Journal of Hydrologic Engineering*, **11:** 555-569. DOI: http://dx.doi.org/10.1061/(ASCE)1084-0699(2006)11:6(555)

Karydas CG, Panagos P, & Gitas IZ. 2014. A classification of water erosion models according to their geospatial characteristics. *International Journal of Digital Earth*, **7**(3): 229-250. DOI: 10.1080/17538947.2012.671380

Kirkby M, Robert J, Irvine B, Gobin A, Govers G, Cerdan O, Tompaey A, Le Bissonnais Y, Daroussin J, King D, Montanarella L, Grimm M, Vieilefont V, Puigdefabregas J, Boer M, Kosmas C, Yassoglou N, Tsara M, Mantel S, Van Lynden G, Hunting J. 2003. Pan-European Soil Erosion Risk Assesment. . *Joint Research Centre, ISPRA*

Kirkby MJ, Gallart F, Kjeldsen TR, Irvine BJ, Froebrich J, Lo Porto A, Team M. 2011. Classifying low flow hydrological regimes at a regional scale. *Hydrology and Earth System Sciences*, **15**(12): 3741-3750. DOI: 10.5194/hess-15-3741-2011

Köppen, W. 1931. Grundriss der Klimakunde. *Walter de Gruyter & Co.*, Berlin

Krysanova V & White M. 2015. Advances in water resources assessment with SWAT—an overview. *Hydrological Sciences Journal*, **60**(5): 771-783. DOI: 10.1080/02626667.2015.1029482

Larned ST, Datry T, Arscott DB, & Tockner K. 2010. Emerging concepts in temporary-river ecology. *Freshwater Biology*, *55*(4), 717-738. DOI: 10.1111/j.1365-2427.2009.02322.x

Le Roux J, Sumner PD, Lorentz SA, Germishuyse T. 2013. Connectivity aspects in sediment migration modelling using the Soil and Water Assessment Tool. *Geosciences*, **3**(1): 1-12 DOI: 10.5923/j.geo.20130301.01

Lesschen JP, Schoorl JM, Cammeraat ELH. 2009. Modelling runoff and erosion for a semi-arid catchment using a multi-scale approach based on hydrological connectivity. *Geomorphology*, **109**: 174-183

Lévesque E, Anctil F, van Griensven A, Beauchamp N. 2008. Evaluation of streamflow simulation by SWAT model for two small watersheds under snowmelt and rainfall. *Hydrological Sciences Joutrnal*, **53**: 961–976

Licciardello F, Rossi CG, Srinivasan R, Zimbone SM. and Barbagallo S, (2011): Hydrologic Evaluation of a Mediterranean Watershed Using the SWAT Model with Multiple PET Estimation Methods. *Transactions of the ASABE*, **54**(5): 1615-1625 ISSN: 0001-2351

Licciardello F, Toscano A, Cirelli GL, Consoli S, and Barbagallo S. 2017. Evaluation of sediment deposition in a Mediterranean reservoir: comparison of long term bathymetric measurements and SWAT estimations. Land Degradation & Development, 28: 566–578, DOI: 10.1002/ldr.2557

Lopez-Vicente M, Navas A, Gaspar L, & Machin J. 2013. Advanced modelling of runoff and soil redistribution for agricultural systems: The SERT model. *Agricultural Water Management,* **125**: 1-12. DOI: 10.1016/j.agwat.2013.04.002

Lu SL, Kayastha N, Thodsen H, van Griensven A, & Andersen HE. 2014. Multiobjective Calibration for Comparing Channel Sediment Routing Models in the Soil and Water Assessment Tool. *Journal of Environmental Quality,* **43**(1): 110-120. DOI: 10.2134/jeq2011.0364

Lu H, Moran CJ, & Prosser IP. 2006. Modelling sediment delivery ratio over the Murray Darling Basin. *Environmental Modelling & Software,* **21**(9): 1297-1308. DOI: http://dx.doi.org/10.1016/j.envsoft.2005.04.021

Marchamalo M, Hooke JM, & Sandercock PJ. 2016. Flow and Sediment Connectivity in Semi-arid Landscapes in SE Spain: Patterns and Controls. *Land Degradation & Development,* **27**(4): 1032-1044. DOI: 10.1002/ldr.2352

Medeiros PHA, Guntner A, Francke T, Mamede GL, de Araùjo JC. 2010. Modelling spatio-temporal patterns of sediment yield and connectivity in a semi-arid catchment with the WASA-SED model. *Hydrological Sciences Journal*, **55**(4): 636-648

Milella P, Bisantino T, Gentile F, Iacobellis V, Trisorio Liuzzi G. 2012. Diagnostic analysis of distributed input and parameter datasets in Mediterranean basin streamflow modeling. *Journal of Hydrology*, **472-473**: 262-276. DOI: 10.1016/j.jhydrol.2012.09.039

Moon J, Srinivasan R, Jacobs JH. 2004. Stream floe estimation using spatially distribuited rainfall in the Trinity River Basin, Texas. *Transaction of the ASABE*, **47**: 1445-1451

Morgan RPC, Quinton JN, Smith RE, Govers G, Poesen JWA, Auerswald K, Styczen ME. 1998. The European Soil Erosion Model (EUROSEM): a dynamic approach for predicting sediment transport from fields and small catchments. *Earth Surface Processes and Landforms*, **23**(6): 527-544. DOI: 10.1002/(SICI)1096-9837(199806)23:6<527::AID-ESP868>3.0.CO;2-5

Moriasi DN, Arnold JG, Van Liew MW, Bingner RL, Harmel RD, & Veith TL. 2007. Model evaluation guidelines for systematic quantification of accuracy in watershed simulations. *Transactions of the ASABE*, **50**(3): 885-900

Muleta MK. 2012. Improving Model Performance Using Season-Based Evaluation. J*ournal of Hydrologic Engineering*, **17**(1): 191-200. DOI: 10.1061/(asce)he.1943-5584.0000421

Nash, J. E., & Sutcliffe, J. V. (1970). River flow forecasting through conceptual models part I — A discussion of principles. *Journal of Hydrology*, **10**(3): 282-290. DOI: http://dx.doi.org/10.1016/0022-1694(70)90255-6

Nash JE & Sutcliffe JV. 1970. River flow forecasting through conceptual models part I — A discussion of principles. *Journal of Hydrology*, **10**(3): 282-290. DOI: http://dx.doi.org/10.1016/0022-1694(70)90255-6

Neitsch SL, Arnold JG, Kiniry JR, Williams JR, King KW. 2002. Soil and Water Assessment Tool Theoretical Documentation. Version 2000. Texas Water Resources Institute, College Station, Texas, USA

Nerantzaki SD, Giannakis GV, Efstathiou D, Nikolaidis NP, Sibetheros IA, Karatzas GP, Zacharias I. 2015. Modeling suspended sediment transport and assessing the impacts of climate change in a karstic Mediterranean watershed. *Science of Total Environment*, **538**: 288-297. DOI: http://dx.doi.org/10.1016/j.scitotenv.2015.07.092

Nikolaidis NP, Bouraoui F, & Bidoglio G. 2013. Hydrologic and geochemical modeling of a karstic Mediterranean watershed. *Journal of Hydrology*, **477**: 129-138. DOI: http://dx.doi.org/10.1016/j.jhydrol.2012.11.018

Oeurng C, Sauvage S, Sanchez-Perez JM. 2011. Assessment of hydrology, sediment and particulate organic carbon yield in a large agricultural catchment using the SWAT model. *Journal of Hydrology*, **401**: 145-153. DOI: doi:10.1016/j.jhydrol.2011.02.017

Oueslati O, De Girolamo AM, Abouabdillah A, Lo Porto A. 2015. Classifying the flow regimes of Mediterranean streams using multi-variate analysis: Classifying the Flow Regimes in Mediterranean Streams. *Hydrological Processes*, **29** (22). DOI10.1002/hyp.10530

Panagos P, Borrelli P, Poesen J, Ballabio C, Lugato E, Meusburger K, Alewell C. 2015. The new assessment of soil loss by water erosion in Europe. *Environmental Science & Policy*, **54**: 438-447. DOI: http://dx.doi.org/10.1016/j.envsci.2015.08.012

Panagos P, Meusburger K, Van Liedekerke M, Alewell C, Hiederer R, & Montanarella L. 2014. Assessing soil erosion in Europe based on data collected through a European network. *Soil Science and Plant Nutrition*, **60**(1): 15-29. DOI: 10.1080/00380768.2013.835701

Pappenberger F & Beven KJ. 2006. Ignorance is bliss: Or seven reasons not to use uncertainty analysis. *Water Resources Research*, **42**(5). DOI: 10.1029/2005WR004820

Parsons JA, 2012. How useful are catchment sediment budgets? *Progress in Physical Geography*, DOI: 10.1177/0309133311424591

Peraza-Castro M, Ruiz-Romera E, Montoya-Armenta LH, Sànchez-Perez JM, Sauvage S. 2015. Evaluation of hydrology, suspended sediment and Nickel loads in a small watershed in Basque Country (Northern Spain) using eco-hydrological SWAT model. *International journal of limnology*, **51**: 59-70. DOI: 10.1051/limn/2015006

Pimentel D. 2006. Soil Erosion: A Food and Environmental Threat. *Environment, Development and Sustainability*, **8**(1): 119-137. DOI: 10.1007/s10668-005-1262-8

Potter C & Hiatt S. 2009. Modeling river flows and sediment dynamics for the Laguna de Santa Rosa watershed in Northern California. *Soil and Water Conservation Society*. **64** (6): 383-393. DOI: 10.2489/jswc.64.6.383

Refsgaard JC, Van der Sluijs JP, Højberg AL, & Vanrolleghem PA. 2007. Uncertainty in the environmental modelling process – A framework and guidance. *Environmental Modelling & Software*, **22**(11): 1543-1556. DOI: http://dx.doi.org/10.1016/j.envsoft.2007.02.004

Rickson RJ. 2014. Can control of soil erosion mitigate water pollution by sediments? *Science of The Total Environment*, **468–469**: 1187-1197. DOI: http://dx.doi.org/10.1016/j.scitotenv.2013.05.057

Romanazzi A, Gentile FG, & Polemio M. 2015. Modelling and management of a Mediterranean karstic coastal aquifer under the effects of seawater intrusion and climate change. *Environmental Earth Sciences*, **74**(1): 115-128. DOI: 10.1007/s12665-015-4423-6

Santhi C, Arnold JG, Williams JR, Dugas WA, Srinivasan R, & Hauck LM. 2001. Validation of the swat model on a large river basin with point and nonpoint sources. *Journal of the American Water Resources Association*, **37**(5): 1169-1188. DOI: 10.1111/j.1752-1688.2001.tb03630.x

Skoulikidis NT, Sabater S, Datry T, Morais MM, Buffagni A, Dörflinger G, Tockner K. 2017. Non-perennial Mediterranean rivers in Europe: Status, pressures, and challenges for research and management. *Science of The Total Environment*, **577**: 1-18. DOI: http://dx.doi.org/10.1016/j.scitotenv.2016.10.147

Smith RE, Goodrich DC, & Quinton JN. 1995. Dynamic, distributed simulation of watershed erosion: The KINEROS2 and EUROSEM models. *Journal of Soil and Water Conservation*, **50**(5): 517-520

Srinivasan R, Arnold JG, Jones CA. 1998. Hydrologic modelling of the United States with the Soil and Water Assessment Tool. *Water Resources Development*, **3**: 312-325

Strauch M, Bernhofer C, Koide S, Volk M, Lorz C, Makeschin F. 2012. Using precipitation data ensemble for uncertainty analysis in SWAT streamflow simulation. *Journal of Hydrology*, **414-415**:413-424. DOI: 10.1016/j.jhydrol.2011.11.014

Theurer FD & Cronshey RG. 1998. *AnnAGNPS - Reach routing processes*. Paper presented at the 1st Federal Interagency Hydrologic Modeling Conference, April 19-23, Las Vegas, NV, USA

Tóth G, Jones A, & Montanarella L. 2013. The LUCAS topsoil database and derived information on the regional variability of cropland topsoil properties in the European Union. Environmental Monitoring and Assessment, **185**(9): 7409-7425. DOI: 10.1007/s10661-013-3109-3

Tibebe D & Bewket W. 2011. Surface runoff and soil erosion estimation using the swat model in the keleta watershed, Ethiopia. *Land Degradation & Development*, **22**(6): 551-564. DOI: 10.1002/ldr.1034

Trombetta A, Iacobellis V, Tarantino E, Gentile F. 2016. Calibration of the AquaCrop model for winter wheat using MODIS LAI images. *Agricultural Water Management*, **164** Part 2: 304-316. DOI: 10.1016/j.agwat.2015.10.013

Uhlenbrook S, Seibert JAN, Leibundgut C, & Rodhe A. 1999. Prediction uncertainty of conceptual rainfall-runoff models caused by problems in identifying model parameters and structure. *Hydrological Sciences Journal*, *44*(5), 779-797. DOI:10.1080/02626669909492273

USDA-ARS. 2011. AGNPS. http://www.ars.usda.gov/Research/docs.htm?docid=5199

USDA-SCS. 1972. National Engineering Handbook, Section 4, Hydrology. *Washington, DC: USDA Soil Conservation Service*

Van Rompaey A, Bazzoffi P, Jones RJA, & Montanarella L. 2005. Modeling sediment yields in Italian catchments. *Geomorphology*, **65**(1-2): 157-169. DOI: 10.1016/j.geomorph.2004.08.006

Verheijen FGA, Jones RJA, Rickson RJ, & Smith CJ. 2009. Tolerable versus actual soil erosion rates in Europe. *Earth-Science Reviews*, **94**(1-4): 23-38. DOI: 10.1016/j.earscirev.2009.02.003

Vigiak O, Malagó A, Bouraoui F, Grizzetti B, Weissteiner CJ, & Pastori M. 2016. Impact of current riparian land on sediment retention in the Danube River Basin. *Sustainability of Water Quality and Ecology*, **8**: 30-49. DOI: http://dx.doi.org/10.1016/j.swaqe.2016.08.001

Vigiak O, Malagó A, Bouraoui F, Vanmaercke M, & Poesen J. 2015. Adapting SWAT hillslope erosion model to predict sediment concentrations and yields in large Basins. *Science of The Total Environment*, **538**: 855-875. DOI: http://dx.doi.org/10.1016/j.scitotenv.2015.08.095

Volk M, Bosch D, Nangia V, & Narasimhan B. 2016. SWAT: Agricultural water and nonpoint source pollution management at a watershed scale. *Agricultural Water Management*, **175**: 1-3. DOI: 10.1016/j.agwat.2016.06.013

Wasowski J, Casarano D, Lamanna C. 2007. Is the current landslide activity in the Daunia region (Italy) controlled by climate or land use change? *Proc. International Conference on "Landslides and Climate Change – Challenges and Solutions"*, Ventnor, UK, 41-49

White ED, Feyereisen GW, Veith TL, Bosch DD. 2009. Improving daily water yield estimates in the Little River watershed: SWAT adjustments Trans. *ASABE*, **52**: 69–79.

Williams JR. 1975. Sediment-yield prediction with Universal Equation using runoff energy factor *Present and Prospective Technology for Predicting Sediment Yield and Sources*, ARS-S-**40**: 244-252: U.S. Dept. Agric

Williams JR & Berndt HD. 1977. Sediment Yield Prediction Based on Watershed Hydrology. **20**(6): DOI: 10.13031/2013.35710

Winchell M, Srinivasan R, Di Luzio M, & Arnold JG. 2013. ArcSWAT Interface for SWAT2012 User's Guide *Blackland Research and Extension Center*, *Temple*, *TXTR*, **439-464**

Wohl E, Bledsoe BP, Jacobson RB, Poff NL, Rathburn SL, Walters DM, & Wilcox AC. 2015. The Natural Sediment Regime in Rivers: Broadening the Foundation for Ecosystem Management. *Bioscience*, **65**(4): 358-371. DOI: 10.1093/biosci/biv002

Yang J, Reichert P, Abbaspour KC, Xia J, & Yang H. 2008. Comparing uncertainty analysis techniques for a SWAT application to the Chaohe Basin in China. *Journal of Hydrology*, **358**(1–2): 1-23. DOI: http://dx.doi.org/10.1016/j.jhydrol.2008.05.012

Zabaleta A, Meaurio M, Ruiz E, & Antiguedad I. 2014. Simulation Climate Change Impact on Runoff and Sediment Yield in a Small Watershed in the Basque Country, Northern Spain. *Journal of Environmental Quality*, **43**(1): 235-245. DOI: 10.2134/jeq2012.0209

Zangh D, Chen X, Yao H, Lin B. 2015. Improved calibration scheme of SWAT by separating wet and dry seasons. *Ecological Modelling* **301**: 54–6

Zema DA, Denisi P, Taguas Ruiz EV, Gòmez JA, Bombino G, Fortunato D. 2016. Evaluation of surface runoff prediction by AnnAGNPS model in a large mediterranean watershed covered by olive groves. *Land Degradation & Development*, **27**: 811-822. DOI: 10.1002/ldr.2390

Table I. A selection of relevant studies performed on the Mediterranean climatic region (classification of Koppen, 1931), concerning sediment load simulation with the SWAT model (this paper included).

Related case studies	Study area	Calibration and Validation Period and time step	Key results
Potter & Hiatt., 2009	California	Few a year grab sample measurements Calibration 2005 - 2007	Average annual sediment load 3.66 t ha^{-1} yr^{-1} SWAT model generally tends to underestimate the measured sediment PBIAS for three gauge station: + 52.6; +26.5 and +73.9
Gamvroudis *et al*., 2014	Greece	Monthly time step Calibration 2010 - 2011	Average annual sediment yield 0.85 t ha^{-1} yr^{-1} In the two main flood event SWAT, simulate suspended sediment appropriately with a slight underestimation. PBIAS for two gauging station: +33.4 and +13.4
Nerantzaki *et al*., 2015	Greece	Monthly time step Calibration: 2011 - 2014	Average erosion rate from 0.97 t ha^{-1} yr^{-1} to 1.6 t ha^{-1} yr^{-1} Model overestimation due to the fact that the majority of the observations had low values of sediment concentration PBIAS -57%
Peraza-Castro *et al*., 2015	Northern Spain	Daily time step Calibration 2009 - 2012 Validation 2001 - 2009	Average annual sediment load 0.33 t ha^{-1} yr^{-1} Underestimation and overestimation during some flood events. The underestimation occurs for four events that according to Montoya-Armenta (2013).
Briak *et al*., 2016	Northern Morocco	Monthly time step Calibration 1976 - 1984 Validation 1985 - 1993	Average annual sediment yield 55 t ha^{-1} yr^{-1} Generally SWAT tends to underestimate peak of sediment concentration PBIAS +7.12 for calibration; PBIAS +15.51 for validation
Gyamfi *et al*., 2016	Southern Africa	Monthly time steps Calibration 1994 - 1995 Validation 1996 - 1997	Mean sediment yield for the Land use change scenario varies from 1.33 t ha^{-1} yr^{-1} to 4.46 t ha^{-1} yr−1. Simulated sediment match fairly with the observed with an underestimation PBIAS + 27.36 for calibration; PBIAS +39.73 for validation
Chen *et al.*, 2017	California	Monthly time step Calibration 2003 - 2008 Validation 2009 - 2014	Model significantly overestimate sediment load during peak events with default Bagnold equation, but produced better results when the physically based Bagnold equation is used. PBIAS - 32 for Calibration; PBIAS 0 for Validation
This Work	Southern Italy	Daily and Monthly time step Calibration 2007-2008 Validation 2009 - 2010	Average annual sediment load 6.8 t ha^{-1} yr^{-1} SWAT model showed generally an overestimation of the dry season and an underestimation of the wet season

Table II. SWAT sensitivity analysis results, default range of parameters and best-fit calibration. Letter R is for relative change (initial parameter is multiplied by 1+ a given value in calibration). Letter V is for replacement (initial parameter is replaced by a given value).

Parameters	Description	t-Stat	p-Value	Range	Best fit
	Runoff				
V__ESCO.hru	Soil Evaporation compensation factor	174.459	0.000	0.83-1.00	1.000
R__CN2.mgt	Curve Number	145.900	0.000	0.04-0.11	0.080
V__ALPHA_BF.gw	Baseflow alpha factor	88.771	0.000	0.38-0.75	0.460
V__GWQMN.gw	Threshold depth of water in shallow aquifer	1.399	0.162	0.19-0.40	0.300
V__GW_REVAP.gw	Groundwater “revap” coefficient	0.934	0.351	0.03-0.14	0.060
V__CH_N2.rte	Manning’s “n” value for main channel	-4.374	0.000	0.01-0.03	0.010
V__CH_K2.rte	Effective hyd. Cond. In the main channel	-17.760	0.000	38.70-42.90	40.910
V__GW_DELAY.gw	Groundwater delay time	-33.269	0.000	31.11-70.37	35.600
V__OV_N.hru	Manning’s “n” value for overland flow	-42.025	0.000	7.51-12.54	12.510
R__SOL_AWC.sol	Soil available water storage capacity	-61.333	0.000	0.39-0.57	0.560
	Sediment				
ADJ_PKR.bsn	Peak rate adjustment factor for sediment routing in the sub-basin	0.087	0.931	-	1.400
LAT_SED.hru	Sediment concentration in groundwater flow	-0.643	0.520	-	250.000
SPCON.bsn	Maximum amount of sediment reentrained during channel sediment routing	-0.672	0.502	-	0.003
BIOMIX.mgt	Biological mixing efficiency	-0.785	0.432	-	0.500

Table III. Model performance statistics for annual calibration/validation and for seasonal calibration (wet/dry periods).

	Calibration			Validation		
	R^2	NSE	PBIAS	R^2	NSE	PBIAS
			Runoff			
Daily	0.6	0.6	-1.0	0.4	0.4	2.0
Monthly	0.9	0.8	12.5	0.6	0.6	-14.3
			Sediment			
Daily	0.6	0.6	-1.5	0.2	0.2	29.5
Monthly	0.7	0.5	-0.6	0.7	0.7	-5.3
	Wet			Dry		
			Runoff			
Daily	0.5	0.5	1.6	0.4	-1.4	-39.8
Monthly	0.6	0.7	-3.6	0.7	-0.3	-43.3
			Sediment			
Daily	0.5	0.5	17.3	0.2	-3.7	-140.1
Monthly	0.7	0.6	-28.2	0.2	0.1	69.0
			Sediment with new calibration			
	Wet (SPCON 0.005)			Dry (SPCON 0.0008)		
Daily	0.5	0.6	-38.4	0.5	0.5	33.9

Table IV. Mean annual sediment yield for each sub-basin as a function of land use, rainfall, soil type, and slope.

Subbasins	Land use	Rainfall (mm)	Soil type	Slope (%) min	Slope (%) max	Sediment Yield ($t\ ha^{-1}\ yr^{-1}$) min	Sediment Yield ($t\ ha^{-1}\ yr^{-1}$) max
1	Winter wheat	578.68	Silty-Clay-Loam/Clay-Loam	0.23	7.18	0.05	1.67
	Olive Groves	578.68	Silty-Clay-Loam/Clay-Loam	8.38	9.20	2.07	2.34
2	Winter wheat	612.28	Silty-Clay/Clay-Loam	0.28	6.45	0.08	1.41
3	Winter wheat	578.68	Silty-Clay-Loam/Clay-Loam	0.25	6.36	0.05	1.06
4	Deciduous Forests	847.4	Clay/Clay-Loam	25.08	27.05	1.7	7.49
	Winter wheat	847.4	Silty-Clay/Silty-Clay-Loam/Clay-Loam	0.25	15.07	0.26	13.83
	Olive Groves	847.4	Clay-Loam	15.04		8.22	
5	Winter wheat	578.68	Silty-Clay/Clay-Loam	4.52	9.48	0.72	2.77
6	Winter wheat	592.84	Clay/Silty-Clay	11.49	11.89	3.08	3.36
7	Winter wheat	578.68	Clay/Silty-Clay/Clay-Loam	7.94	11.40	1.98	3.45
8	Rangeland	592.84	Clay/Clay-Loam	26.85	30.85	0.36	0.79
	Deciduous Forests	592.84	Clay-Loam	28.90		0.11	
	Winter wheat	592.84	Clay/Clay-Loam	16.65	17.46	5.76	6.76
9	Winter wheat	702.8	Clay/Silty-Clay/Clay-Loam	10.19	16.25	5.33	10.61
10	Winter wheat	702.8	Clay/Clay-Loam	12.78	14.41	6.59	8.59
	Deciduous Forests	702.8	Clay/Clay-Loam	19.10	23.97	0.22	0.68
11	Winter wheat	702.8	Silty-Clay-Loam/Clay-Loam	0.14	15.61	0.13	8.75
	Rangeland	702.8	Clay-Loam	18.49		0.25	
	Deciduous Forests	702.8	Clay-Loam	21.62		0.25	
	Beushes and srhubs	702.8	Clay-Loam	0.12	19.76	0.13	0.16
12	Winter wheat	592.84	Clay/Clay-Loam	13.30	16.75	3.52	6.27
	Deciduous Forests	592.84	Clay-Loam	33.40		0.13	
	Beushes and srhubs	592.84	Clay/Clay-Loam	25.87	26.45	0.07	0.25
	Olive Groves	592.84	Clay/Clay-Loam	23.82	26.36	3.21	3.42
13	Deciduous Forests	702.8	Clay-Loam	23.11		0.27	
	Beushes and srhubs	702.8	Clay-Loam	22.49		0.17	
	Winter wheat	702.8	Clay/Clay-Loam	12.64	16.31	5.58	10.3
14	Rangeland	702.8	Clay/Clay-Loam	18.27	18.45	0.25	0.34
	Winter wheat	702.8	Clay/Clay-Loam	15.08	15.22	9.68	9.74
15	Rangeland	592.84	Clay/Clay-Loam	14.60	19.25	0.13	0.3
	Winter wheat	592.84	Clay/Clay-Loam	13.21	14.26	4.19	4.28
16	Rangeland	719.08	Clay/Clay-Loam	21.65	23.00	8.02	13.63
	Deciduous Forests	719.08	Clay-Loam	23.87		1.41	
	Winter wheat	719.08	Clay/Clay-Loam	16.92	18.59	10.67	13.99
	Olive Groves	719.08	Clay-Loam	19.37		12.64	
17	Rangeland	898.88	Clay/Clay-Loam	18.53	20.22	0.57	0.64
	Winter wheat	898.88	Clay/Clay-Loam	14.14	15.08	13.23	15.38